

Lecture notes

-

A mathematical approach to the integer quantum Hall effect

Alex Bols

June 1, 2020

Contents

| | | |
|----------|--|-----------|
| 1 | Introduction | 3 |
| 2 | Discovery of the Quantum Hall Effect | 4 |
| 2.1 | The Classical Hall Effect | 4 |
| 2.2 | Discovery of the integer quantum Hall effect (IQHE) | 6 |
| 3 | Free electrons on the lattice \mathbb{Z}^d | 6 |
| 3.1 | Describing electrons in a crystal | 6 |
| 3.2 | Free electrons | 7 |
| 3.3 | Correspondence between groundstates and Projectors | 8 |
| 3.4 | Single-partice Hamiltonians | 9 |
| 3.5 | Insulators and conductors | 10 |
| 4 | Translation invariant systems | 10 |
| 4.1 | Band insulators and their Fermi projections | 12 |
| 4.1.1 | Exponential decay of correlations | 13 |
| 5 | The Chern number | 14 |
| 5.1 | The Chern number of a single isolated band | 14 |
| 5.2 | The connection 1-form | 15 |
| 5.3 | More bands | 17 |
| 5.4 | The Berry connection | 17 |
| 6 | Locality estimates | 17 |
| 6.1 | Decay of correlations revisited | 18 |
| 6.2 | local lemmas | 19 |

| | | |
|-----------|---|-----------|
| 7 | Quantization of the Hall conductance | 20 |
| 7.1 | An expression for the Hall conductance | 20 |
| 7.2 | The Chern number is the Hall conductance | 22 |
| 7.2.1 | Proof of proposition 7.3 | 22 |
| 7.3 | Proof of proposition 7.4 | 23 |
| 7.4 | Hall plateaux and the role of disorder | 25 |
| 8 | The index of a pair of projections | 26 |
| 9 | Non-commutative Chern number I : | |
| | Flux threading | 27 |
| 9.1 | proofs | 28 |
| 10 | Non-commutative Chern number II : | |
| | Flux piercing | 29 |
| 10.1 | Definitions and results | 30 |
| 10.2 | Proofs | 31 |
| 11 | Equivalence of Chern numbers | 32 |
| 11.1 | Proof of theorem 11.1 | 33 |
| 11.1.1 | Memories of Fredholm | 33 |
| 11.1.2 | Proof sketch | 34 |
| 11.1.3 | Proof of theorem 11.1 | 35 |
| 12 | Bulk-edge correspondence for Hall insulators | 41 |
| 12.1 | The physical picture | 41 |
| 12.2 | A theorem | 43 |
| A | Technicalia | 46 |

1 Introduction

These lecture notes present a rather mathematical approach to understanding the integer quantum Hall effect (IQHE), the remarkable phenomenon that Hall conductances of flat electrical insulators at low temperatures come in multiples of the fundamental constant e^2/h . We will describe the very basic phenomenology in section 2.

It turns out that the IQHE effect can be understood within the framework of the free-electron description of crystals, i.e. in the Hartree-Fock approximation. This framework will be introduced in section 3.

As a first step we will strive to understand the IQHE in translation invariant systems. These systems and their mathematical niceties are introduced in section 4. It will turn out that in this setting the low temperature state of an insulator is mathematically equivalent to a smooth projection-valued map on a two-dimensional base space called the Brillouin zone. To any such map one may associate an integer called the Chern number. Thus we associate Chern numbers to low temperature state of insulators! This is achieved in section 5.

Section 6 is a technical intermezzo locality bounds. These play a crucial role in the proofs to come.

Having associated Chern numbers to two-dimensional insulators it is natural to guess that this Chern number is in fact the Hall conductance. This is shown in section 7.

In section 8 the index of a pair of projections is introduced. This index will be used to extend our understanding of the IQHE to disordered systems (i.e. systems that are not translation invariant).

In the course of showing that the Hall conductance is the Chern number a formula is obtained that doesn't depend on translation invariance. In section 9 we prove that this formula remains integer valued if translation invariance is given up. Thus a *non-commutative* Chern number is discovered.

In section 10 an alternative formulation of the non-commutative Chern number is presented which provides a rigorous version of the famous Laughlin argument. This alternative formulation is shown to be equivalent to the others in section 11.

Finally, in section 12 the so-called bulk-edge correspondence for Hall insulators is introduced. This correspondence says that the edge between two Hall insulators is a (one-dimensional) conductor with the very remarkable property that particles have 'more ways' of travelling in one direction of the edge than in the other. This imbalance is measured by an integer which is equal to the difference of the Chern numbers of the Hall insulators on either side of the edge.

Recommended reading

A mathematical proof is no substitute for a good physical understanding. (It should not come as a surprise that physical understanding historically always comes before mathematical proof). A very good place to seek such understand-

ing is in the lecture notes of David Tong:

- The Quantum Hall Effect - David Tong. These are excellent lecture notes on the physics of both the integer and the fractional quantum Hall effect. They can be found at <http://www.damtp.cam.ac.uk/user/tong/qhe.html>

In the translation invariant case the Hall conductance can be interpreted as the Chern number of a vector bundle. Vector bundles are very interesting mathematical objects. A good introduction can be found in chapter 1 of Allen Hatcher's book:

- Vector bundles & K-theory - Allen Hatcher. Chapter 1 gives the best introduction to vector bundles that I have ever seen. The rest of the book is also great. The book can be found at <https://pi.math.cornell.edu/hatcher/VBKT/VB.pdf>

The phenomenon of Anderson localization is important in understanding the Hall plateaux. A mathematical treatment can be found in

- Random Operators : Disorder Effects on Quantum Spectra and Dynamics - M. Aizenman and S. Warzel.

Errata I'm sure these notes are full of errors. I'd be very happy to hear about any errors you find, you can mail them to alex-b@math.ku.dk.

2 Discovery of the Quantum Hall Effect

The field of topological insulators was born in 1980 when von Klitzing, using samples prepared by Dorda and Pepper, discovered the *integer quantum Hall effect* (IQHE) [9]. Let's explain what that effect is.

2.1 The Classical Hall Effect

The *Hall effect* refers to the phenomenon where perpendicular electric and magnetic fields can induce charge currents *perpendicular* to both fields. This is in contrast to the 'usual' behaviour of conductors, where the charge current is along the electric field which drives it.

Classically, the motion of an electron of charge $-e$ in the presence of an electric field \vec{E} and a magnetic field \vec{B} is governed by the *Lorentz force*

$$\vec{F} = -e\vec{E} - e\vec{v} \times \vec{B} \quad (1)$$

where \vec{v} is the velocity of the electron. Plugging this into Newton's second law we get the equations of motion

$$m \frac{d^2}{dt^2} \vec{x} = -e\vec{E} - e\vec{v} \times \vec{B}. \quad (2)$$

Let us now consider perpendicular fields, say $\vec{E} = E\hat{y}$ in the y -direction and $\vec{B} = B\hat{z}$ in the z -direction. The motion in the z -direction then decouples from the other directions, and the velocity in the z -direction remains constant in time. So we can restrict ourselves to study motion in the xy -plane.

Let's first consider the case where $E = 0$. Then

Exercise 2.1. *the electron moves in circles in the xy -plane with frequency*

$$\omega_B := \frac{eB}{m}. \quad (3)$$

i.e. the general solution is

$$x(t) = X - R \sin(\omega_B t + \phi), \quad y(t) = Y + R \cos(\omega_B t + \phi). \quad (4)$$

The frequency ω_B is called the *cyclotron frequency*. Note that the center and radius of the circular motion are arbitrary, together with the phase they provide four initial conditions to uniquely determine a solution to the equations of motion.

We think of the situation without electric field as describing the system 'at rest', and we now want to see what kind of currents start flowing in response to an electric field. So let's turn on the electric field $\vec{E} = E\hat{y}$, then

Exercise 2.2. *the electron gets an additional velocity $v_{drift} = E/B$ in the x -direction, so the general solution to the equations of motion becomes*

$$x(t) = X - R \sin(\omega_B t + \phi) + v_{drift} t, \quad y(t) = Y + R \cos(\omega_B t + \phi). \quad (5)$$

Remark 2.3. *You can solve this exercise by directly substituting the proposed solution into the equations of motion. A more interesting way to solve it however, is to note that the equations of motion are invariant under Lorentz boosts. You can then boost to a frame where the electric field vanishes, so the motion of the electron in that frame proceeds in circles. Then boosting back to the original frame yields the solution. v_{drift} is then simply the boost velocity needed to get rid of the electric field.*

So, the electron drifts in a direction perpendicular to the applied electric field. To speak of a current we need a finite density of electrons, say ρ per unit area. Then all these electrons drift in the \hat{x} direction with a mean velocity v_{drift} , so we get a current density in the x -direction

$$j_x = -\rho e v_{drift} = -\frac{\rho e}{B} E = -\sigma_{cl} E \quad (6)$$

where we defined the 'classical Hall conductance'

$$\sigma_{cl} = \frac{\rho e}{B}. \quad (7)$$

2.2 Discovery of the integer quantum Hall effect (IQHE)

Slightly rephrasing von Klitzing's result [9], he found that if the Hall conductance is measured in function of the *filling factor* n , i.e. the number of electrons per unit volume, then one finds a dependence illustrated in figure 1. The Hall conductance exhibits *plateaux*, where it takes *quantized values*

$$\sigma_H \in \frac{e^2}{h} \mathbb{Z}. \quad (8)$$

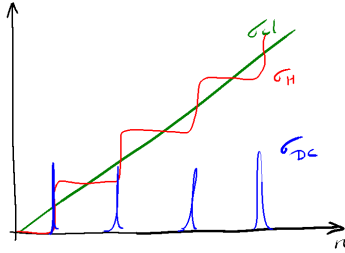


Figure 1: Sketch of von Klitzing's experimental results

For n corresponding to a plateau, the direct conductance of the material vanishes, i.e. the material is an insulator. In between plateaux, the direct conductance is nonzero. This will turn out to be a very significant observation.

3 Free electrons on the lattice \mathbb{Z}^d

We will study a mathematically tractable class of models describing electrons in a d -dimensional crystal. (The only d that are physically relevant are $d = 0, 1, 2, 3$). In $d = 2$ we will be able to find models that exhibit the IQHE.

3.1 Describing electrons in a crystal

We assume that the electrons are tightly bound to the nuclei in the crystal, so that the relevant single-electron states are (close to) the low lying orbitals of the nuclei. The nuclei are assumed to take no part in the dynamics, they are fixed in a crystalline pattern. Therefore, we have a bunch of available orbitals, say N of them, per unit cell of the crystal. i.e. the state space in a single unit cell is a Hilbert space isomorphic to \mathbb{C}^N , with a basis corresponding to low-lying atomic orbitals. The single-particle states of the whole crystal then form the Hilbert space $h = l^2(\mathbb{Z}^d; \mathbb{C}^N)$, where we labelled the unit cells of the crystal by pairs of integers.

A naive definition of the many-body Hilbert space is then

$$\mathcal{H} = \bigoplus_{n \geq 0} \mathcal{H}^{(n)}, \quad \mathcal{H}^{(n)} = h^{\wedge n} \quad (9)$$

where $\mathcal{H}^{(n)}$ is the n -particle space and we allow any number of particles. But this does not suffice for our purposes because we are interested in a finite density of electrons, and therefore require infinitely many electrons when we work in infinite volume. Let us circumvent this problem by considering large but finite volumes. i.e. instead of Z^d we consider a finite lattice of linear dimension L with periodic boundary conditions

$$\Lambda_L := \mathbb{Z}^d / (L\mathbb{Z}^d) \quad (10)$$

i.e. a discrete torus with L^d sites. The single particle hilbert space is then $h_L = l^2(\Lambda_L; \mathbb{C}^N) \cong \mathbb{C}^{L^d \times N}$ and the corresponding many-body Hilbert space

$$\mathcal{H}_L = \bigoplus_{n \geq 0} \mathcal{H}_L^{(n)}, \quad \mathcal{H}_L^{(n)} = h_L^{\wedge n} \quad (11)$$

now does contain states with a finite density of electrons, which simply means a number of electrons proportional to the volume L^d . Note that the direct sum stops at $n = L^d \times N$ because that is the total number of orthogonal one-particles states, and the antisymmetry prohibits two electrons to occupy the same state (the Pauli principle).

3.2 Free electrons

Now that we have a state-space we are left with defining a dynamics, i.e. we must guess what sort of Hamiltonian would give a good description of the electrons in our crystal. Here we will make the rather strong assumption that the electrons don't interact. That non-interacting electrons often do give a good description of crystals is a miracle that goes by the name of Hartree-Fock theory, it is an active field of reseach in mathematical physics. Thus, each individual electron is described by a single particle Hamiltonian $H_L \in \mathcal{L}(h_L)$ and the many-body Hamiltonian is

$$H_L^{(MB)} = \bigoplus_{n \geq 0} H_L^{\otimes n} \in \mathcal{L}(\mathcal{H}_L). \quad (12)$$

We can figure out all the eigenstates and corresponding energies of the many-body Hamiltonian from those of the single-particle Hamiltonian. Indeed, suppose $\{\psi_\alpha\}_{\alpha=1}^{L \times L \times N}$ is a complete set of eigenstates of h_L with

$$h_L \psi_\alpha = \epsilon_\alpha \psi_\alpha. \quad (13)$$

Then it is an easy exercise to show that the ‘Slater determinants’

$$\Psi_{\alpha_1, \dots, \alpha_n} := \psi_{\alpha_1} \wedge \dots \wedge \psi_{\alpha_n} \quad (14)$$

are eigenstates of H_L with

$$H_L \Psi_{\alpha_1, \dots, \alpha_n} = E_{\alpha_1, \dots, \alpha_n} \Psi_{\alpha_1, \dots, \alpha_n}, \quad E_{\alpha_1, \dots, \alpha_n} = \sum_{i=1}^n \epsilon_{\alpha_i}. \quad (15)$$

We get a unique labelling of these eigenstates by demanding $\alpha_1 < \alpha_2 < \dots < \alpha_n$.

3.3 Correspondence between groundstates and Projectors

There is a correspondence between projectors on the single particle Hilbert space and Slater determinants. For an orthonormal set $\{\psi_1, \dots, \psi_n\}$:

$$\psi_1 \wedge \dots \wedge \psi_n \leftrightarrow P = \sum_{i=1}^n |\psi_i\rangle\langle\psi_i|. \quad (16)$$

This correspondence goes a bit further than mere listing of an orthonormal set of states. Indeed for, any ‘single-particle’ observable $O \in \mathcal{L}(h_L)$ we can again form the many-body observable

$$O^{(MB)} = \bigoplus_{n \geq 0} \sum_{i=1}^n \mathbb{1} \otimes \dots \otimes \underbrace{O}_{i^{th} \text{ position}} \otimes \dots \otimes \mathbb{1}. \quad (17)$$

Morally, this asks each particle in the many body state what its value of O is and sums the answers. Then

$$\langle \psi_1 \wedge \dots \wedge \psi_n, O^{(MB)} \psi_1 \wedge \dots \wedge \psi_n \rangle = \text{Tr}\{PO\}. \quad (18)$$

This is nice because we are very often interested in such single particle observables. For example, the operator corresponding to the number of particles sitting in a certain subset $S \subset \Lambda_L$ of the lattice is simply $P_S^{(MB)}$ where P_S is the projector on all single particle states supported in the region S . Moreover, the instantaneous current through the boundary of S is the rate of change of the number of particles in S , so this corresponds to the operator $J_{\partial S}^{(MB)}$ with $J_{\partial S} = dP_S/dt = i[H_L, P_S]$.

Remember from our discussion of von Klitzings’s experiment that we are interested in very low temperature states. We will therefore take the lowest temperature state, i.e. the ground state, of the many-body Hamiltonian to describe the state of our Quantum Hall sample. By the above, we know that this is a Slater determinant and therefore corresponds to a single-particle projector P_F called the *Fermi projector*. Furthermore, we are interested in currents flowing in this state which correspond to one-body observables and can therefore be described completely in the one-particle framework.

This has the happy consequence that we can forget about the difficulties of describing finite density states in infinite volume. The fermi projection remains well defined in infinite volume.

3.4 Single-particle Hamiltonians

It remains to specify what sort of single-particle Hamiltonians on

$$h = l^2(\mathbb{Z}^d; \mathbb{C}^N) \cong l^2(\mathbb{Z}^d) \otimes \mathbb{C}^N \quad (19)$$

we want to consider. Let $\sigma_1, \dots, \sigma_N$ be an ONB of \mathbb{C}^N and denote by $|x, \sigma_i\rangle = |x\rangle \otimes |\sigma_i\rangle$ with $|x\rangle$ the indicator function on $\{x\} \subset \mathbb{Z}^d$. Then the single particle Hamiltonian has matrix elements

$$H_{x,\sigma;y,\sigma'} = \langle x, \sigma | H | y, \sigma' \rangle. \quad (20)$$

We will assume that the Hamiltonian has *finite range*. i.e. there is an $R > 0$ such that

$$H_{x,\sigma;y,\sigma'} = 0, \quad \text{if } |x - y| > R. \quad (21)$$

We call such Hamiltonians ‘of range R ’, or also ‘ R -local’.

Denoting by

$$H_{x,y} = \{H_{x,\sigma_i;y,\sigma_j}\}_{i,j=1,\dots,N} \in \mathbb{C}^{N \times N} \quad (22)$$

we further demand that

$$\|H_{x,y}\| \leq C \quad \text{for all } x, y \in \mathbb{Z}^d. \quad (23)$$

i.e. we want the ‘hopping matrices’ $H_{x,y}$ to be uniformly bounded. Note that $H_{x,y} = 0$ if $|x - y| > R$ by the finite range condition.

Example 3.1. *The discrete Laplacian Δ in d dimensions is the operator on $l^2(\mathbb{Z}^d)$ with matrix elements*

$$\langle x, \Delta y \rangle = \begin{cases} 1 & \text{if } |x - y| = 1 \\ -d & \text{if } x = y \\ 0 & \text{otherwise.} \end{cases} \quad (24)$$

A potential is a multiplication operator V acting on $l^2(\mathbb{Z}^d)$ as

$$V|x\rangle = V(x)|x\rangle \quad (25)$$

for some function $V : \mathbb{Z}^d \rightarrow \mathbb{R}$ that is bounded from below.

Adding a potential to the discrete Laplacian we get the family of discrete Schrödinger operators

$$h = -\Delta + V, \quad (26)$$

these are indeed obtained by discretizing Schrödinger operators on $L^2(\mathbb{R}^d)$.

3.5 Insulators and conductors

Remember that the experimental evidence shows that Hall conductance is quantized if and only if the direct conductance of the material vanishes. i.e. iff the material is an electric insulator. We argue here that an insulator is a material for which the Fermi level lies in a gap in the spectrum of the Hamiltonian. We will keep the discussion very informal. For a better discussion, see any decent book on solid-state physics.

The mechanism of DC conductance is roughly that electrons in the Fermi sea, i.e. single particle states $\psi \in \text{Ran} P_F$, get excited to states $\psi' \perp P_F$ outside the Fermi sea. These excited states accelerate under the influence of an electric field and therefore carry a DC electric current. (The current is finite because these excited electrons scatter against impurities and lattice defects in the crystal. The fact that some disorder does lead to a finite DC conductance is an important open problem of mathematical physics.)

But where do these excitations come from? An important source is *thermal excitations*. As we've discussed, the Fermi projector describes the state of our crystal at zero temperature. In reality, crystals are never at exactly zero temperature, so once in a while our crystal will wander into a state that is not the exact groundstate, but some other state that has slightly higher energy.

The probability of seeing a state of energy ΔE above the groundstate energy is given by the Gibbs distribution $\sim e^{-k_B \Delta E / T}$ with T the temperature and k_B Boltzmann's constant. At $T = 0$ you are sure to be in the groundstate. At $T = \infty$, all states are equally likely. A small but non-zero temperature gives a significant likelihood to states with energies slightly above the groundstate, but almost no probability of very high energy states to occur. So we see that the more low-excitation states there are available, the more states there are that can contribute to DC currents. But if the Fermi energy lies in a gap of the single-particle Hamiltonian, then the first excited state lies at finite energy 2γ above the groundstate. In contrast, if the Fermi energy lies in the bulk of the spectrum of the single-particle Hamiltonian, then there are infinitely many excited states available, lying an arbitrarily small energy above the ground state. Thus, at low but finite temperature, a material with Fermi energy in the gap has almost no states available to participate in DC conductance while a material with Fermi energy in the bulk spectrum has a lot of states available to participate in DC conductance.

We summarise with the slogan *Insulators are gapped, conductors are gapless*.

4 Translation invariant systems

The analysis of the single particle Hamiltonian becomes a lot simpler if we assume translation invariance

$$H_{x,y} = H_{x+r,y+r} =: H_{x-y} \quad (27)$$

for all $x, y, r \in \mathbb{Z}^d$.

Physically, this is not at all unreasonable as crystals tend to be translationally invariant structures. We do miss out on describing the effect of impurities, lattice defect, and of course the edges of the crystal!

All the information about H is now contained in the function $r \mapsto H_r$ or equivalently, in its Fourier transform

$$\tilde{H} : \mathbb{T}^d \rightarrow \mathbb{C}^{N \times N} : k \mapsto \sum_{r \in \mathbb{Z}^d} H_r e^{-ir \cdot k} \quad (28)$$

where $\mathbb{T}^d = \mathbb{R}^d / (2\pi\mathbb{Z}^d)$ is called the *Brillouin torus*. Note that because of the finite range condition, only finitely many of the H_r are nonzero, and $\tilde{H}(k)$ is a very well behaved periodic function on the Brillouin torus.

Solving the eigenvalue problem for all the $\tilde{H}(k)$ is equivalent to solving the eigenvalue problem for the full Hamiltonian H . Indeed, suppose we have for each $k \in \mathbb{T}^d$ an ONB $\{u_\alpha\}_{\alpha=1}^N$ of \mathbb{C}^N such that

$$\tilde{H}(k)|u_\alpha(k)\rangle = \epsilon_\alpha(k)|u_\alpha(k)\rangle. \quad (29)$$

Then the functions

$$\Psi_{\alpha,k} : \mathbb{Z}^d \rightarrow \mathbb{C}^N : x \mapsto e^{ix \cdot k} |u_\alpha(k)\rangle \quad (30)$$

satisfy

$$(H\Psi_{\alpha,k})(x) = \sum_y H_{x,y} \Psi_{\alpha,k}(y) = \sum_y e^{iy \cdot k} H_{x-y} |u_\alpha(k)\rangle \quad (31)$$

$$= \sum_r e^{i(x-r) \cdot k} H_r |u_\alpha(k)\rangle = e^{ix \cdot k} \tilde{H}(k) |u_\alpha(k)\rangle \quad (32)$$

$$= \epsilon_\alpha(k) e^{ix \cdot k} |u_\alpha(k)\rangle = \epsilon_\alpha(k) \Psi_{\alpha,k}(x). \quad (33)$$

i.e. except for the fact that the $\Psi_{\alpha,k}$ are not in $l^2(\mathbb{Z}^d; \mathbb{C}^N)$, they are ‘eigenfunctions’ of H , sometimes called *generalized eigenfunctions*.

All the numbers $\epsilon_\alpha(k)$ appear as energies of these generalized eigenstates, and this means that they are all in the specrum of H (see spectral theory). They also exhaust the spectrum of H because the functions $\Psi_{\alpha,k}$ form a basis of the Hilbert space $l^2(\mathbb{Z}^d; \mathbb{C}^N)$ in the sense of Fourier (see Fourier analysis). i.e. for any $\Phi \in l^2(\mathbb{Z}^d; \mathbb{C}^N)$ we have

$$\Phi(x) = \sum_{\alpha=1}^N \int_{\mathbb{T}^d} dk \tilde{\Phi}_\alpha(k) \Psi_{\alpha,k}(x). \quad (34)$$

Thus $\sigma(H) = \{\epsilon_\alpha(k) | k \in \mathbb{T}^d, \alpha = 1, \dots, N\}$. By relabelling such that $\epsilon_1(k) \leq \epsilon_2(k) \leq \dots \leq \epsilon_N(k)$, the $\epsilon_\alpha(k)$ are continuous functions of k , so we see that H has continuous spectrum (which also follows from the fact that all of its spectrum is associated to generalized eigenfunctions).

4.1 Band insulators and their Fermi projections

What does an insulator look like in this picture? Well, for an insulator there is a gap in the spectrum of H . Therefore the functions $k \mapsto \epsilon_\alpha(k)$ fall in two groups, the ones taking values below the gap and the ones taking values above the gap, see figure 2. Let's suppose that $\epsilon_1, \dots, \epsilon_M$ take values below the gap.

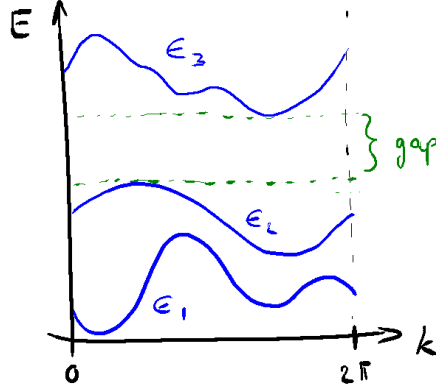


Figure 2: The energy bands of a one-dimensional insulator with a gap between the second and third bands.

The Fermi projector P_F is the orthogonal projector on the subspace of $l^2(\mathbb{Z}^d; \mathbb{C}^N)$ ‘spanned by’ the occupied states $\Psi_{\alpha,k}$ with $k \in \mathbb{T}^d$ and $\alpha = 1, \dots, M$. These states are not actually in the Hilbert space, so what we mean is that P_F projects on (the norm-closure of) all states in $l^2(\mathbb{Z}^d; \mathbb{C}^N)$ whose Fourier expansion (34) only has contributions from those $\Psi_{\alpha,k}$.

Formally, $P_F = \sum_{\alpha=1}^M \int_{\mathbb{T}^d} dk |\Psi_{\alpha,k}\rangle \langle \Psi_{\alpha,k}|$ so its matrix elements are

$$\begin{aligned} \langle x, \sigma | P_F | y, \sigma' \rangle &= \sum_{\alpha=1}^M \int_{\mathbb{T}^d} dk \langle x, \sigma | \Psi_{\alpha,k} \rangle \langle \Psi_{\alpha,k} | y, \sigma' \rangle \\ &= \sum_{\alpha=1}^M \int_{\mathbb{T}^d} dk e^{i(x-y) \cdot k} \langle \sigma | u_\alpha(k) \rangle \langle u_\alpha(k) | \sigma' \rangle \\ &= \int_{\mathbb{T}^d} dk e^{i(x-y) \cdot k} \langle \sigma | \tilde{P}_F(k) | \sigma' \rangle \end{aligned}$$

where we defined

$$\tilde{P}_F(k) := \sum_{\alpha=1}^M |u_\alpha(k)\rangle \langle u_\alpha(k)| \quad (35)$$

the projector on the Bloch vectors of quasi-momentum k with energies below the gap. As for the Hamiltonian we may write

$$(P_F)_{x,y} = \{ \langle x, \sigma_i | P_F | y, \sigma_j \rangle \}_{i,j=1, \dots, N} \quad (36)$$

for the ‘hopping matrix’ from y to x with respect to some basis $\{\sigma_i\}$ of \mathbb{C}^N . We see that, just as for the Hamiltonian,

$$(P_F)_{x,y} = (P_F)_{x+r,y+r} =: (P_F)_{x-y} \quad \text{for all } x, y, r \in \mathbb{Z}^d \quad (37)$$

and

$$\tilde{P}_F(k) = \sum_{r \in \mathbb{Z}^d} (P_F)_r e^{-ir \cdot k}. \quad (38)$$

Thus, while the Hamiltonian is completely described by the function $k \mapsto \tilde{H}(k)$, we see that the Fermi projector is completely described by the function $k \mapsto \tilde{P}_F(k)$, with $\tilde{P}_F(k)$ the projector on the eigenstates of $\tilde{H}(k)$ with energies below the gap. In the next section we will associate to $k \mapsto \tilde{P}_F(k)$ a topologically invariant *Chern number* if $d = 2$. This Chern number correspond to the quantized value of the Hall conductance!

4.1.1 Exponential decay of correlations

Thanks to the gap the map $k \mapsto \tilde{P}_F(k)$ is rather well behaved, in fact it is *analytic*. But $\tilde{P}(k)$ was defined as a Fourier series whose coefficients are the ‘hopping-matrices’ $(P_F)_{x-y} = (P_F)_{x-y}$, see eq. (35). Now, it is a general fact that analytic functions are represented by Fourier series with exponentially decaying coefficients. i.e. we have

$$\|(P_F)_{x,y}\| \leq C e^{-\mu|x-y|} \quad (39)$$

for some constant $C > 0$ and a *correlation length* $\mu > 0$.

This has the following consequence ; Let O_x and O_y be observables on sites $x, y \in \mathbb{Z}^d$, meaning that $O_x = P_x O_x P_x$ and $O_y = P_y O_y P_y$. i.e. an observable on a site x only depends on what the wavefunction looks like at the site x . A good example is the projector P_x , which corresponds in the many-body description to the amount of particles sitting at site x .

We may ask about *correlations* between the observables O_x and O_y in the state P_F . The connected correlation function

$$\langle O_x, O_y \rangle_{P_F} := \text{Tr}\{P_F O_x O_y\} - \text{Tr}\{P_F O_x\} \text{Tr}\{P_F O_y\} \quad (40)$$

is a measure of the statistical dependence between the observables O_x and O_y . i.e. this number is big if knowing the value of O_x teaches you a lot about the value of O_y .

We have as a direct consequence of eq. (39) that the connected correlation functions decay exponentiall with distance:

$$|\langle O_x, O_y \rangle_{P_F}| \leq C \|O_x\| \|O_y\| e^{-\mu|x-y|}. \quad (41)$$

This result can easily be extended to observables supported on sets rather than on single sites. Decay of correlations in the form of eq. (39) play an important role in these lecture notes.

5 The Chern number

We saw that the groundstate of a two-dimensional crystal is completely described by a smooth projection valued map $\mathbb{T}^2 \rightarrow \mathbb{C}^{N \times N} : k \mapsto P(k)$. It turns out that not all such maps can be deformed into each other, i.e. they come with distinct topologies. The topology turns out to be completely characterized by a single integer, the *Chern number*. Two projection valued maps over \mathbb{T}^2 can be deformed into each other (modulo a subtlety which will be mentioned later) if and only if their Chern numbers are the same.

In this section we define the Chern number and show that projection valued maps with different Chern numbers cannot be deformed into each other.

5.1 The Chern number of a single isolated band

If the single particle Hamiltonian H has a gap above the bottom band, then the Fermi projection for Fermi energy in the gap is described by a projection valued map $k \mapsto \tilde{P}(k)$ with $\tilde{P}(k)$ a one-dimensional projection on \mathbb{C}^N .

We call a continuous map $k \mapsto v(k) \in \mathbb{C}^N$ a *section* if $\tilde{P}(k)v(k) = v(k)$ for all k . A section that is nowhere zero is called a *global section*. We will see that not every \tilde{P} admits a global section. The best analogy to this phenomenon is the Möbius band.

Clearly, any global section can be made into a *unit section*, a section $k \mapsto v(k)$ such that $\|v(k)\| = 1$ for all k . (This is because the base space \mathbb{T}^2 is compact). Suppose $k \mapsto \tilde{P}(k)$ admits a global section. We then show that \tilde{P} can be deformed to the trivial projection valued map $k \mapsto P_{\text{triv}}(k) = |e_1\rangle\langle e_1|$. The unit vectors of \mathbb{C}^N form a $2N - 1$ dimensional sphere, so a unit section gives a smooth map from the torus onto this sphere. For $N \geq 2$ all such maps can be contracted to a point ($\pi_{\mathbb{T}^2}(\mathbb{S}^n)$ is trivial for $n \geq 3$), i.e. all unit sections can be deformed to a constant unit section, say $k \mapsto |e_1\rangle$. Such a deformation of a unit-vector valued map gives the desired deformation of \tilde{P} to P_{triv} by simply taking the projection on the range of the unit vector. Conversely, if \tilde{P} is a deformation of P_{triv} then \tilde{P} admits a unit section, just follow the section $k \mapsto |e_1\rangle$ along the deformation.

So to find non-trivial maps $k \mapsto P(k)$ we must find an obstruction to having a unit section. You will show in the exercise session that it is always possible to find a unit section on cylinders, so cover the torus by two open cylinders U^+ and U^- as in figure 3 and let $k \mapsto v^\pm(k) \in \text{Ran} P(k)$ be unit sections on these open cylinders. Let $U^\pm = U^+ \cap U^-$ be the overlap. We can compare the sections on the overlap where they are both defined:

$$g(k) := \langle v^+(k) | v^-(k) \rangle \in U(1). \quad (42)$$

These ‘overlaps’ take values in the unit complex numbers, because both $v_1(k)$ and $v_2(k)$ are unit vectors in the one-dimensional $\text{Ran} P(k)$.

The overlap $U_{1,2}$ is essentially two circles. Let γ be two such circles oriented such that U_1 lies to the left as you walk along γ . Then $g_{1,2}$ gives a map of two circles into the unit complex numbers, which is also a circle. Such a map comes

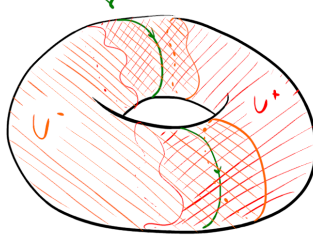


Figure 3: Covering the torus with two open cylinders U^+ and U^- . They overlap in two bands and the path γ consists of two loops circling around those bands.

with a winding number

$$\text{wind}(g) = \frac{1}{2\pi i} \int_{\gamma} \frac{dg}{g} \in \mathbb{Z}. \quad (43)$$

We claim that this number is independent of the way the torus was broken up into cylinders and independent of the choice of unit sections on those cylinders. Thus this winding number is a property of the projection valued map $k \mapsto P(k)$ alone and is called its *Chern number*. Also, if there is a unit section, then this winding number clearly vanishes when computed with respect to that section. Thus, a P with nonzero Chern number does not admit a unit section.

To prove this it is useful to introduce the notion of connection.

5.2 The connection 1-form

Let $\{U_{\alpha}\}$ be an open cover of \mathbb{T}^2 with unit sections v_{α} . This is called a *gauge* because it allows you to describe other sections w.r.t. the chosen sections.

A real-valued connection 1-form is a collection of 1-forms and unit sections $\{\mathcal{A}_{\alpha}, v_{\alpha}\}$ on the $\{U_{\alpha}\}$ that agrees on overlaps. i.e. if the sections v_{α} and v_{β} are related on $U_{\alpha} \cap U_{\beta}$ by

$$v_{\alpha}(k) = t_{\alpha\beta} v_{\beta}(k) \quad (44)$$

then we require

$$\mathcal{A}_{\alpha} = \mathcal{A}_{\beta} - it_{\alpha\beta}^{-1} dt_{\alpha\beta}. \quad (45)$$

The reader might recognize this as a *gauge transformation* of a vector potential in electrodynamics.

To a connection 1-form is associated a curvature 2-form

$$\mathcal{F} = d\mathcal{A}. \quad (46)$$

If you choose different gauges $v'_{\alpha} = \xi v_{\alpha}$ with $\xi \in U(1)$ then the connection 1-form changes according to the gauge transformation

$$\mathcal{A}_{\alpha} \rightarrow \mathcal{A}'_{\alpha} = \mathcal{A}_{\alpha} - i\xi^{-1} d\xi. \quad (47)$$

Two connections are ‘the same’ if they are related by gauge transformations on all patches.

The curvature is gauge invariant

$$\mathcal{F}' = d\mathcal{A}' = d\mathcal{A}. \quad (48)$$

We claim that

$$\text{wind}(g) = \frac{1}{2\pi} \int \mathcal{F} \quad (49)$$

for any choice of connection \mathcal{A} .

Indeed, suppose you have chosen a connection a sections v^\pm on the open cylinders U^\pm and a connection \mathcal{A}_\pm . Let V^\pm be the closed subsets of U^\pm whose boundary is the path γ . Then

$$\int \mathcal{F} = \int_{V^+} \mathcal{F} + \int_{V^-} \mathcal{F} = \int_\gamma (\mathcal{A}_+ - \mathcal{A}_-) \quad (50)$$

by Stoke’s theorem.

But

$$\mathcal{A}_+ - \mathcal{A}_- = -ig^{-1}dg \quad (51)$$

by the compatibility condition (45), which yields the equality (49).

This quantity is independent of the chosen sections v^\pm because the curvature \mathcal{F} is gauge invariant.

To see that it is also independent of the chosen connection, consider the projection valued map $T^2 \times [0, 1] \ni (k, s) \mapsto P(k, s)$ with $P(k, s) = P(k)$ for all s . Choose a connection \mathcal{A} that restricts to connection \mathcal{A}_0 on $\mathbb{T}^2 \times \{0\}$ and restricts to \mathcal{A}_1 on $\mathbb{T}^2 \times \{1\}$. Then the curvature $\mathcal{F} = d\mathcal{A}$ restricts to $\mathcal{F}_0 = d\mathcal{A}_0$ on $\mathbb{T}^2 \times \{0\}$ and restricts to $\mathcal{F}_1 = d\mathcal{A}_1$ on $\mathbb{T}^2 \times \{1\}$ and by Stokes

$$\int_{\mathbb{T}^2} (\mathcal{F}_1 - \mathcal{F}_0) = \int_{\mathbb{T}^2 \times [0, 1]} d\mathcal{F} = 0 \quad (52)$$

because $d\mathcal{F} = d^2\mathcal{A} = 0$.

We can therefore conclude that the number

$$\text{Ch}(P) := \frac{1}{2\pi} \int_{\mathbb{T}^2} \mathcal{F} \in \mathbb{Z} \quad (53)$$

is an integer that depends only on the projection valued map $k \mapsto P(k)$. We call this number the *Chern number* of P .

Finally we note that $\text{Ch}(P)$ changes continuously under smooth changes of P , so since it is also integer valued, it must remain constant under smooth deformations of P . We conclude from this that two projection valued maps P and P' cannot be deformed into each other if they have different Chern numbers.

The converse is also true in the following sense. Two projection valued maps of the same rank and having the same Chern number can be deformed into each other provided the ambient space \mathbb{C}^N has high enough dimension.

5.3 More bands

If the Fermi level lies above M bands then the gapped Fermi projector is described by a projector valued map $\mathbb{T}^2 \ni k \mapsto P(k)$ with $\text{rank} P(k) = M$. We can make a rank-1 map out of this by choosing any orthonormal basis $v_1(k), \dots, v_M(k)$ of $\text{Ran} P(k)$ and then forming the exterior product

$$v_1(k) \wedge \dots \wedge v_M(k) \in \bigwedge \mathbb{C}^N. \quad (54)$$

The map

$$k \mapsto |v_1(k) \wedge \dots \wedge v_M(k)\rangle \langle v_1(k) \wedge \dots \wedge v_M(k)| := P^\wedge(k) \quad (55)$$

is then a smooth projector valued map of rank one and we put

$$\text{Ch}(P) := \text{Ch}(P^\wedge) \in \mathbb{Z}. \quad (56)$$

5.4 The Berry connection

Given a gauge $\{U_\alpha, v_\alpha\}$ for a rank-1 projection-valued map we can construct a connection that will turn out to be useful to do computations and proofs. It is called the Berry connection and it is given by

$$\mathcal{A}_\alpha = i \langle v_\alpha | dv_\alpha \rangle. \quad (57)$$

One easily checks that this is real-valued and satisfies the compatibility relation (45).

In the case of multiple bands a gauge is given by local sections $v_1^{(\alpha)}(k) \wedge \dots \wedge v_M^{(\alpha)}(k)$ and the Berry connections reads

$$\mathcal{A}_\alpha = i \langle v_1^{(\alpha)}(k) \wedge \dots \wedge v_M^{(\alpha)}(k) | dv_1^{(\alpha)}(k) \wedge \dots \wedge v_M^{(\alpha)}(k) \rangle \quad (58)$$

$$= \sum_{i=1}^M i \langle v_i^{(\alpha)} | dv_i^{(\alpha)} \rangle. \quad (59)$$

6 Locality estimates

Locality is an important principle of physics and therefore an important ingredient in saying and proving almost anything interesting about extended physical systems.

The locality structure of our two-dimensional crystal is encoded in the fact the the Hamiltonian is local. We saw that, at least in the translation invariant case, the gapped Fermi projector inherits this locality almost unscathed. We expressed this fact as ‘decay of correlations’. Let’s begin this section by proving that this remains true in absence of translation invariance.

6.1 Decay of correlations revisited

Remember from the translation invariant case that in order to define the Chern number of the Fermi projection we needed the Fourier transform $k \mapsto \tilde{P}(k)$ to be sufficiently well behaved. In fact we saw that $k \mapsto \tilde{P}(k)$ is an analytic map. This regularity manifests itself in real-space as exponential decay of correlations (eq. (39)).

Exponential decay of correlations of gapped Fermi projectors remains true in absence of translation invariance, and it is an important ingredient in proving lemma 10.1. i.e. , just as in the translation invariant case, decay of correlations is instrumental in making the Chern number well defined.

We have

Theorem 6.1. *Let P be the Fermi projector of a gapped Hamiltonian with gap ΔE , then there are numbers $C, \mu > 0$ such that*

$$\|P_{x,y}\| \leq C e^{-\mu|x-y|} \quad (60)$$

where $P_{x,y} = P_x P P_y$. The number μ is called the correlation length and it depends linearly on the gap ΔE .

Proof : This is an application of the Combes-Thomas estimate on the resolvent of the Hamiltonian: (see for example section 10.3 of [2]).

$$\|(z - H)_{x,y}^{-1}\| \leq \frac{2}{\text{dist}(z, \sigma(H))} \exp(-\alpha \text{dist}(z, \sigma(H)) |x - y|) \quad (61)$$

for some constant $\alpha > 0$ that depends on H .

We write the Fermi projector as a Riezs projection

$$P = \frac{1}{2\pi i} \oint_{\gamma} dz (z - H)^{-1} \quad (62)$$

where γ is a path in \mathbb{C} circling the occupied spectrum in a counterclockwise direction, and keeping a distance $\Delta E/2$ from $\sigma(H)$. Using the Combes-Thomas estimate we get

$$\|P_{x,y}\| \leq \frac{1}{2\pi} \int_{\gamma} dz \|(z - H)_{x,y}^{-1}\| \quad (63)$$

$$\frac{C}{\Delta E} e^{-\alpha \Delta E |x-y|} \quad (64)$$

where we used that the path γ has a finite length. \square

One can speculate how much the decay of correlations may be weakened without losing the Chern number. The Chern number of a projection-valued map clearly remains well defined if $k \mapsto \tilde{P}(k)$ is merely sufficiently differentiable (rather than analytic). If $k \mapsto \tilde{P}(k)$ is d -times differentiable then there is algebraic decay of correlations $\|P_{x,y}\| \leq C |x - y|^{d+1}$.

This line of thought is relevant for understanding *topological phase transitions*. Fix a Fermi energy μ and a Hamiltonians H with a gap at μ . If this Hamiltonian is continuously deformed while keeping the gap at μ open, then the Chern number of the corresponding Fermi projection remains constant. The only way in which the Chern number of the Fermi projector can change as a result of continuous change of the parent Hamiltonian is if the gap closes. When the gap closes the Fermi projection no longer has exponential decay of correlations. In fact its correlations must decay so slowly that the Chern number is no longer well-defined!

6.2 local lemmas

We give definitions and lemmas relating to the locality of operators. Most of these are obvious, or at least they are rigorous expressions of intuitive facts. It turns out however that sometimes some nasty technical footwork is needed to prove the obvious.

The gapped Fermi projection is a prime example of a *local* operator:

Definition 6.2. *An operator A is (exponentially) local if*

$$\|P_x A P_y\| \leq C e^{-\mu|x-y|} \quad (65)$$

for some $C, \mu > 0$.

Definition 6.3. *An operator A is local and supported near a set S if*

$$\|P_x A P_y\| \leq C e^{-\mu(|x-y| + \text{dist} x, S)} \quad (66)$$

for some $C, \mu > 0$

and where $\text{dist}(x, S) := \min\{|x - y| \mid y \in S\}$.

Clearly

Lemma 6.4. *If A, B are local then so are AB and $\alpha A + \beta B$ for any $\alpha, \beta \in \mathbb{C}$.*

Proof : Exercise. □

For a set S we denote by $\partial S := \{x \in S \mid \text{dist} x, S^c \leq 1\}$ the *boundary* of S . We denote by $\Lambda_S = \sum_{x \in S} P_x$ the projector on the region S .

We capture the fact that if P is a local projector (like a Fermi projector), then far from ∂S the operator $P \Lambda_S P$, and in fact any power of it, still looks like a projector.

Lemma 6.5. *If P is a local projector then $A = (P \Lambda_S P)^2 - P \Lambda_S P$ is local and supported near ∂S .*

Proof : We write

$$A = P \Lambda_S P (P \Lambda_S P - P) = -P \Lambda_S P \Lambda_{S^c} P \quad (67)$$

from which the statement immediately follows. \square

In section 9 we will be interested in a unitary of the form $e^{2\pi i P \Lambda_S P}$. The exponent looks like a projection far from ∂S so we expect that the exponential looks like the identity far from ∂S . Indeed (see Proposition 4.4. in [6])

Lemma 6.6. *Let $A = P \Lambda_S P$ for a local projector P , then*

$$e^{2\pi i A} - \mathbb{1} \quad (68)$$

is local and supported near ∂S .

Proof : Write

$$\begin{aligned} e^{2\pi i A} - \mathbb{1} &= P e^{2\pi i A} P - P e^{2\pi i \Lambda_S} P \\ &= \sum_{n \geq 2} \frac{(2\pi i)^n}{n!} (A^n - A). \end{aligned}$$

Then note that

$$A^n - A = (A^2 - A) (A^{n-2} - A^{n-3} + \dots + (-1)^n \mathbb{1}). \quad (69)$$

Now if $\|A_{x,y}\| \leq C e^{-\mu|x,y|}$ then $\|A_{x,y}^k\| \leq C^k e^{-\mu|x-y|}$ by the triangle inequality (this isn't entirely trivial), so the second factor has matrix elements bounded by $n C^n e^{-\mu|x-y|}$. The first factor is local and supported near ∂S by lemma 6.5. Plugging all this into the above we get a finite sum and therefore prove the claim. \square

7 Quantization of the Hall conductance

In this section we give a definition of the Hall conductance and show that it is equal to the Chern number of the Fermi projection. We follow [1].

7.1 An expression for the Hall conductance

We want to drive a Hall current by applying a unit electric potential drop along the 2-direction, leading to an electric field which we will take to live in the strip $S_L^{(2)} := \{(x_1, x_2) \in \mathbb{Z}^2 \mid |x_2| \leq L\}$, see figure 4. Such a field is produced by a potential

$$v : \mathbb{Z}^2 \rightarrow \mathbb{R} : (x_1, x_2) \mapsto \begin{cases} x_2/(2L) & \text{if } |x_2| \leq L \\ 1/2 & \text{if } x_2 > L \\ -1/2 & \text{if } x_2 < -L. \end{cases} \quad (70)$$

We imagine that we turn on this field over time, so the Hamiltonian at time t is given by

$$H(t) = H + e^{\delta t} \eta V \quad (71)$$

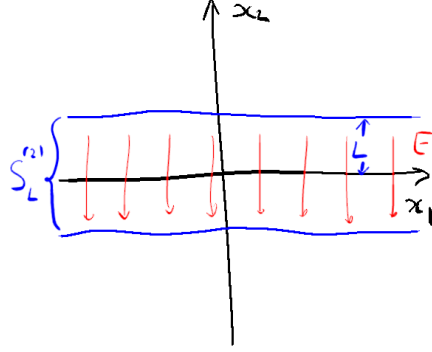


Figure 4: The electric field driving the Hall current lives in a strip.

where $V = \hat{v}$ is the multiplication operator corresponding to the potential (70), and we end up with a potential drop η at time $t = 0$. We are interested in doing this very slowly, so $\delta \rightarrow 0^+$.

We expect that this potential drives a Hall current in the 1-direction. Let's measure this current across the line $x_1 = 0$, then this current corresponds to the rate of change in the number of particles in the positive-1 half-plane. i.e. if Λ_1 is the projector on this half plane then, in the Heisenberg picture,

$$J = \frac{d\Lambda_1}{dt} = -i[H, \Lambda_1]. \quad (72)$$

To know what the current at time $t = 0$ is we must know the state $\rho(0)$ at time 0. The state at time t is the unique solution to

$$\frac{d\rho(t)}{dt} = i[H(t), \rho(t)] \quad (73)$$

with boundary condition $\rho(-\infty) = P$. The current at time $t = 0$ is then

$$j_H = \text{Tr}\{\rho(0)J\}. \quad (74)$$

In the linear-response approximation we are interested in very weak fields, i.e. $\eta \ll 1$. Using Duhamel's formula, we get

$$\rho(0) - P = -i \int_{-\infty}^0 dt e^{\delta t} \eta e^{itH} [V, P] e^{-itH} + \mathcal{O}(\eta^2) \quad (75)$$

to first order in η . Hence, noting also that $\text{Tr}\{PJ\} = 0$ are led to the following definition:

Definition 7.1. *The Hall Conductance is*

$$\sigma_H = \frac{j_H}{\eta} = -\lim_{\delta \downarrow 0} \text{Tr} \left\{ \int_{-\infty}^0 dt e^{\delta t} e^{-itH} [H, \Lambda_1] e^{itH} [V, P] \right\}. \quad (76)$$

This is called the *Kubo formula* [10].

7.2 The Chern number is the Hall conductance

We now show that the Hall conductance is equal to the Chern number.

Theorem 7.2. *The Chern number is the Hall conductance:*

$$\sigma_H = \frac{\text{Ch}(P)}{2\pi}. \quad (77)$$

Proof: A direct consequence of the two propositions 7.3 and 7.4 below. \square

The two propositions are

Proposition 7.3. *The Hall conductance may be expressed as*

$$\sigma_H = i \text{Tr}\{P[[P, \Lambda_1][P, \Lambda_2]]\} \quad (78)$$

Proposition 7.4. *The Chern number of P may also be expressed as*

$$\text{Ch}(P) = \text{Ch}_I(P) := 2\pi i \text{Tr}\{P[[P, \Lambda_1][P, \Lambda_2]]\}. \quad (79)$$

Remark 7.5. *These two propositions show that*

$$2\pi i \text{Tr}\{P[[P, \Lambda_1], [P, \Lambda_2]]\} \quad (80)$$

is integer-valued, and may take non-zero values corresponding to non-trivial Hall conductance if P is a translation invariant gapped Fermi projector. But the formula still makes sense for a non-translationally invariant Fermi projector P with exponential decay of correlations. One might hope that it remains integer valued in this more general setting. This will be shown in the next section, and in another way in sections 10 and 11.

7.2.1 Proof of proposition 7.3

The Hilbert-Schmidt operators \mathcal{L}^2 form a Hilbert space with inner product $\langle A, B \rangle = \text{Tr}\{A^\dagger B\}$. The map

$$\text{ad}_H : \mathcal{L}^2 \rightarrow \mathcal{L}^2 : O \mapsto [H, O] \quad (81)$$

is self-adjoint and has resolvent

$$(\text{ad}_H - i\delta)^{-1}(O) = -i \int_{-\infty}^0 dt e^{\delta t} e^{-itH} O e^{itH} \quad (82)$$

for any $\delta > 0$. We recognize this in the formula (76) for the Hall conductance, except that the resolvent acts on $\text{ad}_H(\Lambda_1)$ which is not Hilbert-Schmidt.

We get around this as follows ; first we write $[V, P] = P[V, P]P^\perp + P^\perp[V, P]P$ and use cyclicity of the trace to get

$$\sigma_H = -\lim_{\delta \downarrow 0} \text{Tr} \left\{ \int_{-\infty}^0 dt e^{\delta t} e^{-itH} [H, [[\Lambda_1, P], P]] e^{itH} [V, P] \right\}. \quad (83)$$

We then decompose the identity as $\mathbb{1} = \sum_{x \in \mathbb{Z}^2} P_x$ to obtain

$$\sigma_H = i \lim_{\delta \downarrow 0} \sum_x \text{Tr} \{ (\text{ad}_H - i\delta) \text{ad}_H ([[\Lambda_1, P], P] P_x) [V, P] \} \quad (84)$$

where one may check using decay of correlations that $[[\Lambda_1, P], P] P_x$ is a Hilbert-Schmidt operator for all x . The functional calculus for ad_H now applies and we get

$$\sigma_H = -i \text{Tr} \{ [[\Lambda_1, P], P] [V, P] \} = i \text{Tr} \{ P [[\Lambda_1, P], [V, P]] \}. \quad (85)$$

The result follows by noting that we could have done this entire argument with a sharp potential $V = \Lambda_2$, and that the original potential is a convex combination of translates of such a sharp potential (and an identity). \square

7.3 Proof of proposition 7.4

To work with $\text{Ch}(P)$ we choose a gauge $\{U_\alpha, \wedge_{i=1}^M u_i^{(\alpha)}\}$ for the rank-1 map P^\wedge giving a Berry connection

$$\mathcal{A}^{(\alpha)} = \sum_{i=1}^M i \langle u_i^{(\alpha)}, du_i^{(\alpha)} \rangle \quad (86)$$

with curvature

$$\mathcal{F} = d\mathcal{A} = \sum_i \left(\langle \partial_{k_1} u_i^{(\alpha)}, \partial_{k_2} u_i^{(\alpha)} \rangle - \{1 \leftrightarrow 2\} \right) dk_1 dk_2 \quad (87)$$

so

$$\text{Ch}(P) = \frac{1}{2\pi i} \int_{\mathbb{T}^2} \mathcal{F}. \quad (88)$$

Consider the commutator

$$J_1 := i[P, X_1] \quad (89)$$

(We call this J_1 because it is the current generated by the ‘Hamiltonian’ P). It has translation invariant hopping matrices

$$P_x [P, X_1] P_y = -(x_1 - y_1) P_{x-y} \quad (90)$$

so we can take its Fourier transform

$$\tilde{J}_1(k) = -i \sum_r r_1 P_r e^{-ir \cdot k} = \partial_{k_1} \tilde{P}(k). \quad (91)$$

The same is of course true for the other coordinate direction:

$$\tilde{J}_2(k) = \partial_{k_2} \tilde{P}(k). \quad (92)$$

But

$$\tilde{P}(k) = \sum_{i=1}^M |u_i\rangle \langle u_i| \quad (93)$$

(where we dropped the superscript α) so after a short calculation we find

$$\mathrm{Tr}\{\tilde{P}[\tilde{J}_1, \tilde{J}_2]\} = \sum_{i=1}^M (\langle \partial_{k_1} u_i, \partial_{k_2} u_i \rangle - \{1 \leftrightarrow 2\}), \quad (94)$$

precisely the $U(1)$ -curvature (87)! i.e. we found

$$\mathrm{Ch}(P) = \frac{1}{2\pi i} \int_{\mathbb{T}^2} dk_1 dk_2 \mathrm{Tr}\{\tilde{P}(k)[\tilde{J}_1(k), \tilde{J}_2(k)]\}. \quad (95)$$

Now, using the fact that if A, B are translation invariant operators we have

$$\tilde{A}(k)\tilde{B}(k) = \widetilde{AB}(k) \quad (96)$$

and

$$\frac{1}{2\pi} \int_{\mathbb{T}^2} dk_1 dk_2 \mathrm{tr} \tilde{A}(k) = 2\pi \mathrm{Tr} P_{x_0} A P_{x_0} \quad (97)$$

for any $x_0 \in \mathbb{Z}^2$, we get (using cyclicity of the trace)

$$\mathrm{Ch}(P) = -2\pi i \mathrm{Tr}\{P_{x_0} P[J_1, J_2]\} \quad (98)$$

$$= 2\pi i \mathrm{Tr}\{P_{x_0} P[[P, X_1], [P, X_2]]\}. \quad (99)$$

Now consider the ‘elementary switch functions’

$$\theta_a : \mathbb{R} \rightarrow \mathbb{R} : x \mapsto \begin{cases} 1 & \text{if } x \geq a \\ 0 & \text{otherwise.} \end{cases} \quad (100)$$

By translation invariance

$$\begin{aligned} & \mathrm{Tr}\{P[[P, \theta_a(X_1)], [P, \theta_b(X_2)]]\} \\ &= \frac{1}{(2L+1)^2} \sum_{a,b \in [-L, L]} \mathrm{Tr}\{P[[P, \theta_a(X_1)], [P, \theta_b(X_2)]]\}. \end{aligned}$$

Pulling the sum through the trace and the commutators, (and noting that subtracting $[P, (2L+1)\mathbb{1}] = 0$) this becomes

$$\frac{1}{(2L+1)^2} \mathrm{Tr}\{P[P, \Lambda_L(X_1)], [P, \Lambda_L(X_2)]\} \quad (101)$$

where

$$\Lambda_L(x) = \begin{cases} x & \text{if } |x| \leq L \\ L & \text{if } x > L \\ -L & \text{if } x < -L. \end{cases} \quad (102)$$

It now remains to show that

$$\lim_{L \uparrow \infty} \frac{1}{(2L+1)^2} \mathrm{Tr}\{P[[P, \Lambda_L(X_1)], [P, \Lambda_L(X_2)]]\} = \mathrm{Tr}\{P_0 P[[P, X_1], [P, X_2]]\}. \quad (103)$$

We shall only sketch the proof of this. By decay of correlations

$$P_x[P, \Lambda_L(X_1)]P_y \approx 0 \quad (104)$$

if x or y is outside of the strip $S_1 := \{(x_1, x_2) \in \mathbb{Z}^2 \mid |x_1| \leq L\}$. The corresponding fact is true for the $P_x[P, \Lambda_L(X_2)]P_y$ and it follows that

$$P_x[[P, \Lambda_L(X_1)], [P, \Lambda_L(X_2)]]P_y \approx 0 \quad (105)$$

if x or y is outside of the square $\Delta = S_1 \cap S_2$. Hence, for L large, and again by decay of correlations

$$\begin{aligned} \text{Tr}\{P[[P, \Lambda_L(X_1)], [P, \Lambda_L(X_2)]]\} &\approx \sum_{x_0 \in \Delta} \text{Tr}\{P_{x_0}P[[P, \Lambda_L(X_1)], [\Lambda_L(X_2)]]\} \\ &\approx (2L+1)^2 \text{Tr}\{P_0P[[P, X_1], [P, X_2]]\}. \end{aligned} \quad (106)$$

Dividing through by the volume $(2L+1)$ then yields the claim for elementary switch functions. Noting that any switch function is a convex combination of the elementary ones then yields the claim for general switch functions. \square

7.4 Hall plateaux and the role of disorder

We now have some understanding of how a quantized Hall current appears in insulators. There remains a large gap in our understanding however. The experiment shows that the Hall conductance is quantized for most values of the filling factor. A translation invariant system is an insulator only for filling factors that precisely fill all energy levels up to a gap, i.e. almost never!

The mechanism responsible for the Hall plateaux is *Anderson localization*. This is the phenomenon where a disordered potential causes particles with energies near the edge of the spectrum to ‘get stuck’. Put in another way, if H is a translation invariant Hamiltonian and V is a random potential, perhaps due to impurities in the crystal, then the spectrum of $H + \lambda V$ looks as in figure 5. The energies near the edges of the perturbed bands are now true eigenvalues of $H + \lambda V$ with eigenvectors that are exponentially localized!

If the filling factor is such that the Fermi level lies in such a region of anderson localized spectrum, then the corresponding Fermi projector still has exponential decay of correlations and we may hope that we can still associate an integer Chern number to it, equal to the Hall conductance. This program can indeed be carried out. In these lecture notes we only focus on one aspect of this program, namely understanding the Hall conductance for disordered systems with gap, i.e. getting rid of translation invariance.

All relevant facts about Anderson localization are collected and proven in the excellent book [2]. Quantization of the Hall conductance when the Fermi energy lies in a region of Anderson Localized spectrum is proven in [4, 1] and many other places.

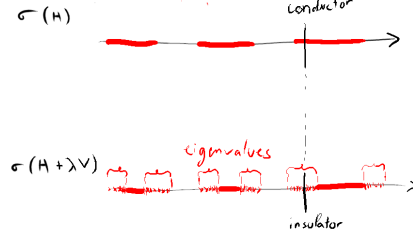


Figure 5: Disorder localizes the spectrum at the edges of bands.

8 The index of a pair of projections

The index of a pair of projections was introduced in [3] with the purpose of understanding the IQHE.

Theorem 8.1. *Let P and Q be orthogonal projections on a separable Hilbert space \mathcal{H} such that their difference $A = Q - P$ is compact. Then*

$$\text{index}(Q, P) := \dim \ker(A - \mathbb{1}) - \dim \ker(A + \mathbb{1}) \in \mathbb{Z}, \quad (108)$$

called the index of the pair of projections (Q, P) , is stable under norm continuous deformations of P and Q .

Moreover, if $A \in \mathcal{L}^p(\mathcal{H})$ (i.e. A^p is trace class) for some odd $p \in \mathbb{N}$, then

$$\text{index}(Q, P) = \text{Tr } A^p. \quad (109)$$

Proof: The result follows by noting a spectral symmetry of A . Note first of all that A , being a difference of orthogonal projections, satisfies $\|A\| \leq 1$. We assumed that A is compact, so its spectrum consists of eigenvalues $\lambda_i \in [-1, 1]$, possibly accumulating at 0.

Denote by E_λ the projector onto the λ -eigenspace of A . We will show that $\dim E_\lambda = \dim E_{-\lambda}$ whenever $|\lambda| < 1$. To that end, introduce the operator $B = Q - P^\perp$ and note two remarkable identities:

$$\{A, B\} := AB + BA = 0 \quad (110)$$

and

$$A^2 + B^2 = \mathbb{1}. \quad (111)$$

Take $\psi \in E_\lambda$ with $|\lambda| < 1$. Then, using eq. (110)

$$AB\psi = -BA\psi = -\lambda B\psi. \quad (112)$$

So if we can guarantee that $B\psi \neq 0$ then we have found a nontrivial $B\psi \in E_{-\lambda}$. Indeed, using eq. (111) we get

$$B^2\psi = (\mathbb{1} - A^2)\psi = (1 - \lambda^2)\psi \neq 0 \quad (113)$$

and therefore $B\psi \neq 0$. Hence B is an *injective* linear map from E_λ to $E_{-\lambda}$. But, by the same argument, B is also an injective map from $E_{-\lambda}$ to E_λ . It follows that E_λ and $E_{-\lambda}$ have the same dimension.

Now, let $P(t)$ be norm-continuous such that $A(t) = Q - P(t)$ is compact for all t . Take a sequence $t_n \rightarrow t^*$ and suppose the largest eigenvalue of $A(t^*)$ not equal to one is $1 - \epsilon_+$ and the smallest eigenvalue of $A(t^*)$ not equal to -1 is $-1 + \epsilon_-$. Take n large enough such that $\|A(t_n) - A(t^*)\| < \min\{\epsilon_+, \epsilon_-\}/8$, then

$$\dim E_1(A(t_n)) + \sum_{\lambda \in (1-\epsilon_+/4, 1)} \dim E_\lambda(A(t_n)) = \dim E_1(A(t^*)) \quad (114)$$

and

$$\dim E_{-1}(A(t_n)) + \sum_{\lambda \in (-1, -1+\epsilon_-/4)} \dim E_\lambda(A(t_n)) = \dim E_{-1}(A(t^*)). \quad (115)$$

But by the spectral symmetry just shown,

$$\sum_{\lambda \in (1-\epsilon_+/4, 1)} \dim E_\lambda(A(t_n)) = \sum_{\lambda \in (-1, -1+\epsilon_-/4)} \dim E_\lambda(A(t_n)) \quad (116)$$

Hence

$$\dim E_1(A(t_n)) - \dim E_{-1}(A(t_n)) = \dim E_1(A(t^*)) - \dim E_{-1}(A(t^*)) \quad (117)$$

i.e. $\text{index}(P(t_n), Q) = \text{index}(P(t^*), Q)$. So $\text{index}(P(t), Q)$ is continuous at t^* . Since t^* was arbitrary, $\text{index}(P(t), Q)$ is continuous everywhere and therefore constant. Continuous changes of Q are dealt with in exactly the same way. \square

9 Non-commutative Chern number I : Flux threading

In the presence of disorder the theory of vector bundles is not available to us. However, our investigation of the Hall conductance led to a good candidate formula (see proposition 7.4) for a Chern number that makes sense in the non-translation invariant case. If this *non-commutative Chern number* indeed remains quantized, it extends the Chern number obtained via the theory of vector bundles. Roughly following appendix C of Kitaev's [8], we show now that this is indeed the case.

Theorem 9.1. *Let P be a gapped Fermi projector, then*

$$\text{Ch}_I(P) := i \text{Tr}\{P[[P, \Lambda_1], [P, \Lambda_2]]\} \in \mathbb{Z}. \quad (118)$$

The proof of this theorem is rather interesting. We will interpret the integer as a quantity of particles pumped through the system by a certain unitary U that leaves the Fermi projection invariant $[U, P] = 0$.

Proof : To prove the theorem we consider the unitary $U = e^{2\pi i P \Lambda_2 P}$ which we interpret as the result of threading a unit of magnetic flux over the x_1 -axis.

The unitary U acts as the identity for away from the x_1 -axis. This is because far away from the x_1 -axis the exponent is close to 0 or P , but $e^0 = e^{2\pi i P} = \mathbb{1}$. On top of that, U is a quasi-local operator because $P \Lambda_2 P$ is (by decay of correlations of P). Indeed, it is shown in lemma 6.6 that $U - \mathbb{1}$ is local and supported near the x_1 -axis. It follows from this fact that

Lemma 9.2.

$$U^\dagger \Lambda_1 U - \Lambda_1 \quad (119)$$

is trace-class.

Therefore

$$\text{flow}(U) := \text{Tr}\{U^\dagger \Lambda_1 U - \Lambda_1\} \in \mathbb{Z} \quad (120)$$

because it is the index of a pair of projections. We interpret this integer as the number of particles transported across the line $x_1 = 0$ by the flux threading process modelled by U .

Λ_1 models all the available states sitting in the positive-1 half plane, but we expect the transport of particles to happen within the groundstate space P . Indeed

Lemma 9.3. *We have*

$$\text{flow}(U) = \text{Tr}\{U^\dagger P \Lambda_1 P U - P \Lambda_1 P\}. \quad (121)$$

Now we can compute

$$\begin{aligned} \text{flow}(U) &= \text{Tr}\{U^\dagger P \Lambda_1 P U - P \Lambda_1 P\} \\ &= \int_0^{2\pi} d\phi \text{Tr} \left\{ \frac{d}{dt} (e^{-i\phi P \Lambda_2 P} P \Lambda_1 P e^{i\phi P \Lambda_2 P}) \right\} \\ &= i \text{Tr}\{[P \Lambda_1 P, P \Lambda_2 P]\}. \end{aligned}$$

A final computation yields

$$i \text{Tr}\{[P \Lambda_1 P, P \Lambda_2 P]\} = i \text{Tr}\{P[[P, \Lambda_1], [P, \Lambda_2]]\} \quad (122)$$

proving the theorem. \square

9.1 proofs

Proof of lemma 9.2 : Note that $U^\dagger \Lambda_1 U - \Lambda_1 = U^\dagger [\Lambda_1, U]$ so it is sufficient to show that $[\Lambda_1, U] = [\Lambda_1, U - \mathbb{1}]$ is trace-class. But we know from lemma 6.6 that $A = U - \mathbb{1}$ is local and supported near the x_1 -axis.

If x is in the positive-1 half-plane then

$$[\Lambda_1, A] P_x = \Lambda_1^\perp P P_x \quad (123)$$

Hence $P_y[\Lambda_1, A]P_x$ is non-zero only if y is in the negative- x_1 half-plane. Together with the locality of A this shows that $[\Lambda_1, A]\Lambda_1$ is supported near the x_2 -axis. The same argument shows that $[\Lambda_1, A]\Lambda_1^{perp}$ and hence $[\Lambda_1, A]$ is supported near the x_2 -axis. Because A is supported near the x_1 -axis we have then that $[\Lambda_1, A]$ is supported near the origin, i.e.

$$\|P_x[\Lambda_1, A]P_y\| \leq Ce^{-\mu(|x-y|+|x|)}. \quad (124)$$

It follows then from lemma A.1 that $[\Lambda_1, A]$ is trace class, proving the lemma. \square

Proof of lemma 9.3 : We have

$$\begin{aligned} \text{flow}(U) &= \text{Tr}\{U^\dagger P\Lambda_1 P U - P\Lambda_1 P\} \\ &\quad + \text{Tr}\{U^\dagger \bar{\Lambda}_1 U - \bar{\Lambda}_1\}. \end{aligned}$$

where $\bar{\Lambda}_1 = P\Lambda_1 P^\perp + P^\perp \Lambda_1 P$ is the off-diagonal part of Λ_1 . We rewrite the second trace as

$$\text{Tr}\{(U^\dagger - \mathbb{1})[\bar{\Lambda}_1, U - \mathbb{1}]\} \quad (125)$$

where we noted that

$$\text{Tr}\{[\bar{\Lambda}_1, U - \mathbb{1}]\} = 0 \quad (126)$$

Indeed, letting $S_i^r = \{(x_1, x_2) \mid |x_i| \leq r\}$ be the strip of width $2r$ around the x_i -axis then

$$\lim_r \|P_{S_1^r} \bar{\Lambda}_1 P_{S_1^r} - \bar{\Lambda}_1\| = 0 \quad (127)$$

and

$$\lim_r \|P_{S_2^r}(U - \mathbb{1})P_{S_2^r} - (U - \mathbb{1})\| = 0 \quad (128)$$

hence

$$\text{Tr}\{[\bar{\Lambda}_1, U - \mathbb{1}]\} = \lim_r \text{Tr}\{[P_{\Delta^r} \bar{\Lambda}_1 P_{\Delta^r}, P_{\Delta^r}(U - \mathbb{1})P_{\Delta^r}]\} = 0 \quad (129)$$

where $\Delta^r = S_1^r \cap S_2^r$ is the square of with $2r$ centered at the origin.

Writign $A = U - \mathbb{1}$, we use the same trick on equation (125) to get

$$\text{Tr}\{A^\dagger [\bar{\Lambda}_1, A]\} = \lim_r \text{Tr}\{(P_{S_1^r}[A^d ag, A]P_{S_1^r} P_{\Delta^r} \bar{\Lambda}_1 P_{\Delta^r})\} = 0 \quad (130)$$

because $[A^\dagger, A] = 0$. This concludes the proof. \square

10 Non-commutative Chern number II : Flux piercing

In this section we follow [3] to give a rigorous version of the Laughlin argument [11].

10.1 Definitions and results

Let's take intuition from the physics. Suppose we slowly pierce our material with a unit of magnetic flux : $\phi(t)$ with $\phi(0) = 0$ and $\phi(T) = 2\pi$. This will induce an electric field E as in figure 6, and hence a Hall current flowing radially towards or away from the locus of flux insertion.

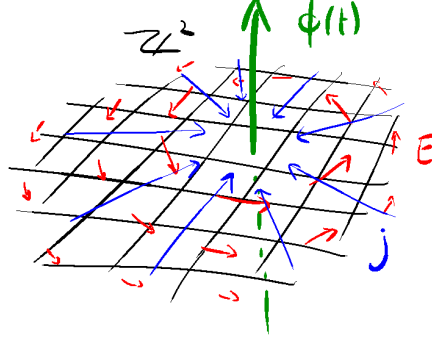


Figure 6: Piercing flux through a two-dimensional Hall insulator leads to Hall currents flowing radially.

Very far from the location of flux insertion the electric field is very weak and the adiabatic principle tells us that the Fermi Projection doesn't change much there. (This means that, if $P(t)$ is the Fermi projection describing the state of our crystal at time t , then $\text{Tr}\langle P(t)O \rangle$ is almost constant for observables O supported far away from the location of flux insertion.)

However, in the vicinity of the flux tube we will be left with some excess charge. The amount of charge is proportional to the Hall conductance and is therefore quantized. Thus we want to compare the amount of particles in $P(T)$ with the amount of particles in $P(0)$.

Given a Fermi projector P it is a rather difficult task to figure out what is the corresponding $P(T)$ obtained by adiabatically piercing a unit of flux. But since the phenomenon we seek is essentially topological and therefore robust, we don't need to be so accurate, we can just go with a simple inspired guess for what $P(T)$ should look like.

We will take out Fermi projector P and model flux piercing at $a \in \mathbb{R}^2 \setminus \mathbb{Z}^2$ by

$$U_a |x, \sigma\rangle = e^{i\theta_a(x)} |x, \sigma\rangle \quad (131)$$

for all $x \in \mathbb{Z}^2$. Here $\theta_a(x)$ is the angle the vector $x - a$ makes with the 1-axis. See figure 7.

To understand that this models flux piercing, notice that *locally* $x \mapsto \theta_a(x)$ can be interpreted as an electric potential whose gradient is precisely the electric field which is generated by the flux tube, see figure 7.

We then transform the Fermi projector to

$$Q = U^\dagger P U. \quad (132)$$

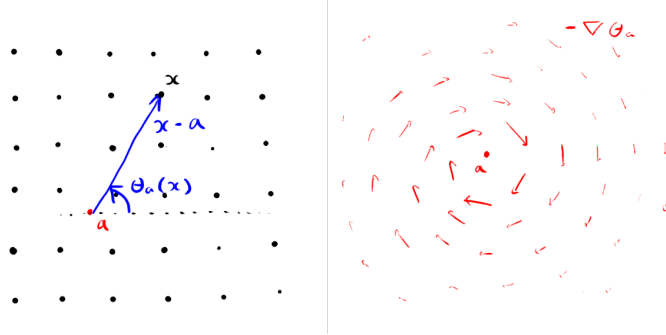


Figure 7: Definition of the ‘potential’ θ_a and a picture of the electric field it generates.

We want to compare the amount of particles in the state represented by Q with the amount of particles in the original state represented by P . The total amount of particles contained in a Slater-determinant state represented by Fermi projector P is just the trace $\text{Tr } P$. This is infinite for both P and Q , But we are interested in the difference

$$\text{Tr}\{Q - P\} \quad (133)$$

which we wish to interpret as the amount of particles pulled towards to locus of flux piercing.

For this to make sense, $A = Q - P$ should be trace class. It turns out that it is not. We are however saved by the index of a pair of projections, see theorem 8.1. This theorem allows us to interpret $\text{index}(Q - P)$ as the number of particles pulled towards the locus of flux piercing as long as $Q - P$ is compact! In fact we have

Lemma 10.1. *The operator A is compact. Moreover, A^3 is trace class.*

This allows us to define:

Definition 10.2. *The Chern number of a gapped Fermi projection P is*

$$\text{Ch}_{II}(P) := \text{index}(U^\dagger P U, P) = \text{Tr}(U^\dagger P U - P)^3 \in \mathbb{Z} \quad (134)$$

where U_a is the flux piercing operator defined in eq. (131).

$\text{Ch}_{II}(P)$ Does not depend on $a \in \mathbb{R}^2 \setminus \mathbb{Z}^2$ because continuously moving a leads to norm-continuous change in U_a and therefore norm-continuous change of $U^\dagger P U$, and the index of projections is stable under norm-continuous changes of the projections.

10.2 Proofs

Proof of lemma 10.1 :

We will use lemma A.1, so we want to bound the hopping matrices

$$A_{x,y} = P_x (U^\dagger P U - P) P_y = \left(e^{i(\theta_a(y) - \theta_a(x))} - 1 \right) P_{x,y}. \quad (135)$$

For x and y far apart this is small because of decay of correlations (theorem 6.1). For x and y close together but far from a this is small because then $\theta_a(x) - \theta_a(y)$ is close a multiple of 2π , leading to

$$\left| e^{i(\theta_a(y) - \theta_a(x))} - 1 \right| \leq c \frac{|x - y|}{|y - a|} \quad (136)$$

for some constant $c > 0$. It follows from this that

$$\|A_{x+r,x}\| \leq C \frac{|r|}{|a - x|} e^{-\mu|r|} \quad (137)$$

for some $C > 0$, where we used exponential decay of correlations

Using the fact that $\|\cdot\|_3 \leq \|\cdot\|$ we then get from lemma A.1 and decay of correlations that

$$\|A\|_3 \leq \sum_r C |r| e^{-\mu|r|} \left(\sum_x \frac{1}{|a - r|^3} \right)^{1/3}. \quad (138)$$

Now,

$$\sum_x \frac{1}{|a - x|^3} < \infty \quad (139)$$

is summable, and so is

$$\sum_r |r| e^{-\mu|r|} < \infty. \quad (140)$$

We conclude that

$$\|A\|_3 < \infty \quad (141)$$

so A^3 is trace class. \square

11 Equivalence of Chern numbers

In the translation invariant case we associated to a gapped Fermi projector P a smooth projector valued map $\mathbb{T}^2 \rightarrow \text{Proj}_M(\mathbb{C}^N) : k \mapsto \tilde{P}$, and with this map in turn a Chern number $\text{Ch}(P) \in \mathbb{Z}$. We showed in section 7 that this Chern number is equal to 2π times the Hall conductance, and we found a local expression:

$$2\pi \sigma_H = \text{Ch}(P) = \text{Ch}_I(P) = 2\pi i \text{Tr}\{P[[P, \Lambda_1][P, \Lambda_2]]\}. \quad (142)$$

In section 9 we showed that the ‘non-commutative’ Chern number $\text{Ch}_I(P)$ remains integer valued even if translation invariance is lost.

In the previous section we associated to any gapped Fermi projector yet another integer

$$Ch_{II}(P) = \text{index}(U_a^\dagger P U_a, P). \quad (143)$$

Becacause we could interpret both $\text{Ch}_I(P)$ and $\text{Ch}_{II}(P)$ as an anout of charge moved by a Hall current it is reasonable to conjecture that they are actually the same integer. Indeed

Theorem 11.1. *Let P be a gapped Fermi projection, then*

$$\text{Ch}_{II}(P) = \text{Ch}_I(P). \quad (144)$$

It follows in particular that, for a translation invariant gapped Fermi projector, $\sigma_H = \text{Ch}(P) = \text{Ch}_{II}(P)$.

11.1 Proof of theorem 11.1

This theorem is usually proven in the translation invariant case using the ‘Connes area formula’ [1, 4, 3]. We choose to give a more ‘physical’ proof that does not require translation invariance.

11.1.1 Memories of Fredholm

We summarise the main facts about Fredholm operators, these facts will be used freely in the rest of this section. See [12] for a brief readable introduction.

Let \mathcal{H} be a separable Hilbert space. A bounded operator F acting on \mathcal{H} is Fredholm if its kernel and cokernel are finite dimensional. We denote the space of all Fredholm operators on \mathcal{H} by $\mathcal{F}(\mathcal{H})$.

If $F \in \mathcal{F}(\mathcal{H})$ then we define its *index* to be

$$\text{index}(F) := \dim \ker F - \dim \text{coker } F. \quad (145)$$

The index is norm-continuous, i.e. if $t \mapsto F(t)$ is a norm-continuous path of Fredholm operators, then they all have the same index.

If F is Fredholm and K is compact, then $F + K$ is Fredholm with the same index as F .

We can write the non-commutative chern number as a Fredholm index:

Proposition 11.2. *We have*

$$\text{index}(U_a^\dagger P U_a, P) = -\text{index}(P U_a P + P^\perp). \quad (146)$$

Proof : Write $Q = U_a^\dagger P U_a$. We have to show that

$$\dim \ker(Q - P + \mathbb{1}) = \dim \ker(P U_a P + P^\perp) \quad (147)$$

and

$$\dim \ker(Q - P - \mathbb{1}) = \dim \text{coker}(P U_a P + P^\perp). \quad (148)$$

To show the former, take $\psi \in \ker(Q - P + \mathbb{1})$. Then $(Q + P^\perp)\psi = 0$ hence $\langle \psi | Q | \psi \rangle = -\langle \psi | P^\perp | \psi \rangle$. But P^\perp and Q are non-negative operators, hence $P\psi = \psi$ and $Q\psi = 0$. Conversely, if $P\psi = \psi$ and $Q\psi = 0$ then $\psi \in \ker(Q - P + \mathbb{1})$, i.e.

$$\ker(Q - P + \mathbb{1}) = \{\psi \mid P\psi = \psi, Q\psi = 0\}. \quad (149)$$

Now take $\psi \in \ker(PU_a^\dagger P + P^\perp)$. Then clearly $P\psi = \psi$ and $0 = PUP\psi = PU\psi$. By multiplying with U^\dagger we get $Q\psi = 0$. Conversely, if $P\psi = \psi$ and $Q\psi = 0$ then $\psi \in \ker(PU_a P + P^\perp)$, i.e.

$$\ker(PU_a P + P^\perp) = \{\psi \mid P\psi = \psi, Q\psi = 0\}. \quad (150)$$

Thus we have shown the first equality. The second one is shown in exactly the same way. \square

Finally we mention Fedosov's formula (see for example [5] for proofs)

Proposition 11.3. *Let F be a bounded operator on \mathcal{H} . If $(\mathbb{1} - F^*F) \in \mathcal{L}^p$ and $(\mathbb{1} - FF^*) \in \mathcal{L}^p$ for some $p \in [1, \infty)$ then F is a Fredholm operator with index*

$$\mathrm{Tr} \{(\mathbb{1} - F^*F)^p\} - \mathrm{Tr} \{(\mathbb{1} - FF^*)^p\}.$$

11.1.2 Proof sketch

Let us represent the flux-piercing unitary U_a by lines flowing towards the locus of flux insertion a as in panel A of figure 8. The lines are level sets of the function θ_a and they come with arrows, indicating that the flux piercing generates a Hall current along those lines. Let's call the lines 'flow lines'. The Chern number is the Fredholm index of $F_A = PU_a P + P^\perp$.

In a first step we deform U_a so that the flow lines are restricted to a wedge as in panel B of figure 8. This is achieved by deforming θ_a to a function $\hat{\theta}_a$ that is (mod 2π) constant outside the wedge. We get a new Fredholm operator $F_B = P\tilde{U}P + P^\perp$ with $\tilde{U}P_x = e^{i\hat{\theta}_a(x)}P_x$. This deformation can be done in a continuous way, so the Fredholm index is stable: $\mathrm{index} F_A = \mathrm{index} F_B$.

Now suppose we chose the 1-coordinate of a to be very large. Remember, the Chern number measures how much charge is piled up near the point a . Almost all of this charge is then contained in the positive-1 half-plane, so we can sandwich with the half-space projector Λ_1 to obtain $F_C = \Lambda_1 F_B \Lambda_1 + \Lambda_1^\perp$. This is depicted in panel C of figure 8. The operator F_C will be shown to be Fredholm and $F_C - F_B$ will be shown to be compact, so $\mathrm{index} F_B = \mathrm{index} F_C$.

Now we introduce an opposite flux at $-a$, see panel D of figure 8. Mathematically, we modify F_C to obtain a new Fredholm operator F_D by introducing a potential for the opposite flux also. This opposite flux lives far outside of Λ_1 so it does not affect the Fredholm index.

Finally, we pull the flux tube out of the plane, allowing a current to flow through the $x_1 = 0$ line. We are then left with the situation depicted in panel E of figure 8. Now the flow-lines are the level sets of a globally defined potential

$2\pi\xi$ going from 0 in the negative-2 half-plane to 2π in the positive-2 half-plane.
i.e. we have a Fredholm operator

$$F_E = \Lambda_1(Pe^{2\pi i\xi}P + P^\perp)\Lambda_1 + \Lambda_1^\perp. \quad (151)$$

Finally, we argue that we can raise P up in the exponent after which the potential ξ can be deformed to the sharp potential Λ_2 , obtaining

$$F_F = \Lambda_1 e^{2\pi P\Lambda_2 P} \Lambda_1 + \Lambda_1^\perp \quad (152)$$

with the same index. But the Fredholm index of F_F is again the index of a pair of projections:

$$\text{index} F_F = \text{index}(e^{2\pi i P\Lambda_2 P} \Lambda_1 e^{-2\pi i P\Lambda_2 P}, \Lambda_1) \quad (153)$$

$$= \text{Tr}\{e^{2\pi i P\Lambda_2 P} \Lambda_1 e^{-2\pi i P\Lambda_2 P} - \Lambda_1\} \quad (154)$$

$$= \text{Ch}_I(P) \quad (155)$$

where the last equality was already obtained in the proof of theorem 9.1.

11.1.3 Proof of theorem 11.1

Before embarking on the proof, we introduce some notation. For any function $f : \mathbb{Z}^2 \rightarrow \mathbb{C}$ we denote by \hat{f} the multiplication operator defined by $\hat{f}P_x = f(x)P_x$. Recalling the function θ_a we take its exponent $u_a = e^{i\theta_a}$ and then we have

$$U_a = \hat{u}_a. \quad (156)$$

Proof : Step 1

We start with the non-commutative Chern number, which we noted above can be written as a Fredholm index

$$\text{Ch}_{II}(P) = \text{index}(F_A) \quad (157)$$

with $F_A = PU_aP + P^\perp$ and U_a the flux piercing operator defined by

$$U_a P_x = e^{i\theta_a(x)} P_x \quad (158)$$

with $\theta_a(x) \in [0, 2\pi)$ the angle of the vector $x - a$ with the 1-axis.

We now continuously deform the function θ_a to the functions $\theta_{t,a}$ taking values

$$\theta_{t,a}(x) = \begin{cases} 0 & \text{if } \theta_a(x) \in [0, t] \\ 2\pi & \text{if } \theta_a(x) \in [2\pi - t, 2\pi] \\ 4(\theta_a(x) - t) & \text{otherwise.} \end{cases} \quad (159)$$

We have $\theta_a = \theta_{0,a}$ and $t \mapsto \theta_{t,a}(x)$ continuous for all x . This leads to a continuous deformation of u_a to $u_{t,a} = e^{i\theta_{t,a}}$ and hence a norm-continuous deformation $U_a = \hat{u}_a$ to $U_{t,a} = \hat{u}_{t,a}$. The $u_{t,a}$ satisfy the condition of lemma 11.4 for all $t \in [0, 3\pi/4]$ so we get a norm-continuous path of Fredholm operators

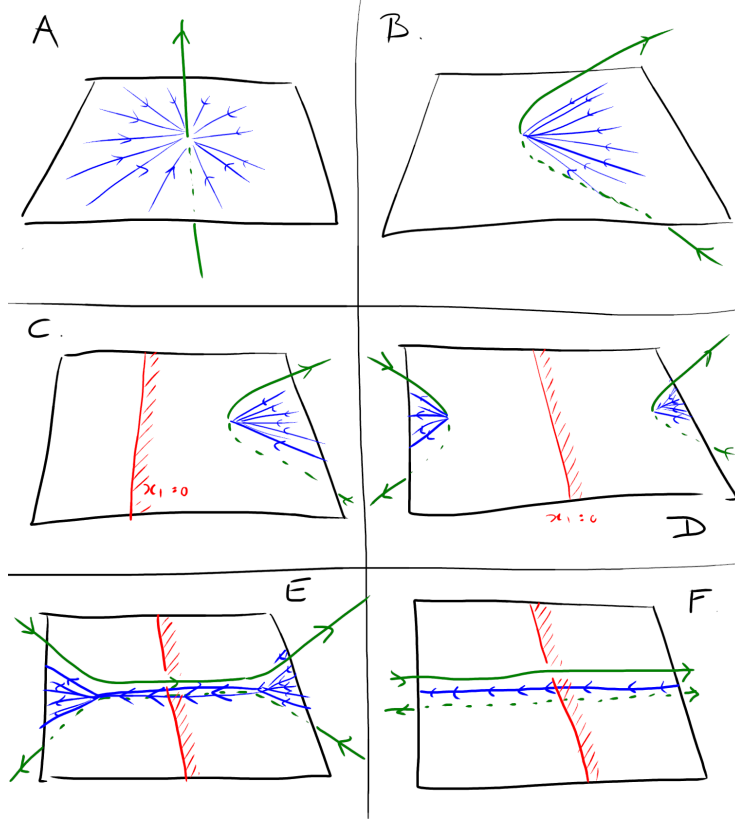


Figure 8: The deformations for the proof of theorem 11.1

$F_A(t) = PU_{t,a}P + P^\perp$, and we put $F_B = F_A(3\pi/4)$. By stability of the Fredholm index under norm-continuous deformations we have

$$\text{index} F_B = \text{index} F_A. \quad (160)$$

Step 2

We now assume that we have chosen $a = (a_1, 0)$ with $a_1 \ll 0$. We have of course

$$F_B = \Lambda_1 F_B \Lambda_1 + \Lambda_1 F_B + \Lambda_1^\perp + \Lambda_1^\perp F_B \Lambda_1 + \Lambda_1^\perp F_B \Lambda_1^\perp \quad (161)$$

where Λ_1 is the projector on the negative-1 halfspace. We will now show that the second and third terms in this expression, the ones that ‘couple’ Λ_1 to Λ_1^\perp , are \mathcal{L}^3 and in particular compact. Then since compact perturbations of Fredholm operators are still Fredholm with the same index, we have

$$\text{index} F_B = \text{index} (\Lambda_1 F_B \Lambda_1 + \Lambda_1^\perp F_B \Lambda_1^\perp). \quad (162)$$

Let’s show it for the second term, the third term is dealt with in exactly the

same way. We have $\Lambda_1 F_B \Lambda_1^\perp = \Lambda_1 (F_B - \mathbb{1}) \Lambda_1^\perp$ but

$$F_B - \mathbb{1} = P[\hat{u}_{3\pi/4,a}, P] + P(\hat{u}_{3\pi/4,a} - \mathbb{1}). \quad (163)$$

Here the first term is \mathcal{L}^3 by lemma 11.4. Sandwishing the second term between Λ_1 and Λ_1^\perp has the factor $(\hat{u}_{3\pi/4,a} - \mathbb{1}) \Lambda_1^\perp = 0$ so we indeed have that $\Lambda_1 F_B + \Lambda_1^\perp \in \mathcal{L}^3$.

By exactly the same reasoning we have that $\Lambda_1^\perp (F_B - \mathbb{1}) \Lambda_1^\perp \in \mathcal{L}^3$, so we get from eq. (162) that

$$\text{index} F_B = \text{index} F_C \quad (164)$$

with $F_C = \Lambda_1 F_B \Lambda_1 + \Lambda_1^\perp$.

Step 3

We now insert an opposite flux as in panel D of figure 8. The opposite flux will not change our Fredholm index because it is inserted far away from the half-plane onto which Λ_1 projects.

The opposite flux is modelled by a unitary \hat{v} with

$$v(x_1, x_2) = u_{3\pi/4,a}(-x_1, x_2). \quad (165)$$

Inserting both fluxes therefore corresponds to the product $\hat{u}_{3\pi/4,a} \hat{v}$ and the operator corresponding panel D of figure 8 is

$$F_D = \Lambda_1 (P \hat{u}_{3\pi/4,a} \hat{v} P + P^\perp) \Lambda_1 + \Lambda_1^\perp. \quad (166)$$

We claim that the difference

$$F_D - F_C = \Lambda_1 P \hat{u}_{3\pi/4,a} (\hat{v} - \mathbb{1}) P \Lambda_1 \quad (167)$$

is compact. This is so because

$$(\hat{v} - \mathbb{1}) P \Lambda_1 \quad (168)$$

is compact. Indeed, $\hat{v} - \mathbb{1}$ is non-zero only on the cone

$$C = \{x \mid \theta_{-a}(x) \in [-\pi/4, \pi/4]\}. \quad (169)$$

On this cone the function $v - 1$ is bounded and using the exponential decay of correlations we have for $x \in C$

$$\sum_r \|P_x (\hat{v} - \mathbb{1}) P \Lambda_1 P_{x+r}\|_1 \leq C e^{-\mu|x_1|} \quad (170)$$

because r must bridge the gap between $x \in C$ and the negative-1 half-plane. Then we get

$$\sum_x \left(\sum_r \|P_x (\hat{v} - \mathbb{1}) P \Lambda_1 P_{x+r}\|_1 \right) < \infty \quad (171)$$

so $(\hat{v} - \mathbb{1})P\Lambda_1$ is trace class by lemma A.1. The trace class operators form a two-sided ideal in the bounded operators so also $F_D - F_C = \Lambda_1 P \hat{u}_{3\pi/4,a} (\hat{v} - \mathbb{1}) P \Lambda_1$ is trace class and therefore compact. It follows that F_D is Fredholm with

$$\text{index} F_D = \text{index} F_C. \quad (172)$$

Step 4

We can write $u_{3\pi/4,a} v = e^{2\pi i \xi}$ with exponent

$$\xi(x_1, x_2) = \begin{cases} \theta_{3\pi/4,a}(x_1, x_2) & \text{if } x_1 \leq 0 \\ \theta_{3\pi/4,a}(-x_1, x_2) & \text{if } x_1 > 0. \end{cases} \quad (173)$$

so

$$F_D = \Lambda_1 (P e^{2\pi i \hat{\xi}} P + P^\perp) \Lambda_1 + \Lambda_1^\perp. \quad (174)$$

We now raise the projector P in the exponent. To that end let $v_t = e^{2\pi i (\mathbb{1} - tP^\perp) \hat{\xi} (\mathbb{1} - tP^\perp)}$ and

$$V_t = P v_t P + P^\perp \quad \text{and} \quad F_t = \Lambda_1 V_t \Lambda_1 + \Lambda_1^\perp \quad (175)$$

then $F_0 = F_D$ and

$$F_E := F_1 = \Lambda_1 e^{iP \hat{\xi} P} \Lambda_1 + \Lambda_1^\perp. \quad (176)$$

Note that $Q_t = \mathbb{1} - tP^\perp$ and ξ satisfy the hypotheses of lemma 11.5, so $[P, v_t] \in \mathcal{L}^5$ for all t .

The map $t \mapsto F_t$ is clearly norm-continuous, we shall now show that all F_t are Fredholm. By Fedosov's formula, it is sufficient to show that $\mathbb{1} - F_t^* F_t$ and $\mathbb{1} - F_t F_t^*$ are \mathcal{L}^3 . We show this here for $\mathbb{1} - F_t^* F_t$, the other case is completely analogous.

From a short computation it follows that

$$\mathbb{1} - F_t^* F_t = \Lambda_1 (\mathbb{1} - V_t^* V_t) \Lambda_1 - \Lambda_1 ([\Lambda_1, V_t^*] [\Lambda_1, V_t]) \Lambda_1. \quad (177)$$

Here we have

$$\mathbb{1} - V_t^* V_t = -P [P, v_t] [P, v_t^*] P \quad (178)$$

which is \mathcal{L}^3 because $[P, v_t] \in \mathcal{L}^3$. It thus remains only to deal with the second term of (177), which we will do by showing that $[\Lambda_1, V_t] \in \mathcal{L}^3$. In order to do that, we show that both $\Lambda_1 V_t \Lambda_1^\perp$ and $\Lambda_1^\perp V_t \Lambda_1$ are in \mathcal{L}^3 . We show this only for the first of these, the proof for the other being entirely analogous.

We have

$$\Lambda_1 V_t \Lambda_1^\perp = \Lambda_1 ([P, v_t] P + (v_t - \mathbb{1}) P) \Lambda_1^\perp. \quad (179)$$

Since $[P, v_t] \in \mathcal{L}^3$ it remains only to deal with the term $\Lambda_1 (v_t - \mathbb{1}) P \Lambda_1^\perp$.

Since Q_t and ξ satisfy the hypothesis of lemma 11.5, we can follow the proof of that lemma to obtain

$$\| (e^{iQ_t \hat{\xi} Q_t} - e^{i\hat{\xi}(n) Q_t^2}) P \|_{nm} = e^{-\mu'' |n-m|} \times \mathcal{O}(|n|^{-1}). \quad (180)$$

Now we use the fact that $PQ_t = P$, hence $Pe^{i\hat{\xi}(n)Q_t^2} = Pe^{i\hat{\xi}(n)}$ to obtain

$$\|(e^{iQ_t\hat{\xi}Q_t}P - e^{i\hat{\xi}(n)}P)_{nm}\|_1 = e^{-\mu''|n-m|} \times \mathcal{O}(|n|^{-1}). \quad (181)$$

But $e^{i\hat{\xi}(n)} = \mathbb{1}$ for all n outside the double cone Γ , hence

$$\|((v_t - \mathbb{1})P)_{nm}\|_1 = e^{-\mu''|n-m|} \times \mathcal{O}(|n|^{-1}) \quad (182)$$

for $n \notin \Gamma$.

Now then, we decompose

$$\Lambda_1(v_t - \mathbb{1})P\Lambda_1^\perp = \Lambda_+(v_t - \mathbb{1})P\Lambda_1^\perp + \Lambda_1(\mathbb{1} - \Lambda_+^\perp)(v_t - \mathbb{1})P\Lambda_1^\perp. \quad (183)$$

The second term is \mathcal{L}^3 by (182) and the locality of v_t and P . The first term is \mathcal{L}^1 because $\Lambda_+\Lambda_1^\perp = 0$ and $(v_t - \mathbb{1})P$ is local. This concludes the proof that all F_t are Fredholm, so we have obtained

$$\text{index}F_E = \text{index}F_D. \quad (184)$$

Step 5

Finally, as already noted in the sketch of proof,

$$\begin{aligned} \text{index}F_E &= \text{Tr}\{e^{-2\pi i P\hat{\xi}P}P\Lambda_1Pe^{2\pi i\hat{\xi}} - P\Lambda_1P\} \\ &= i \text{Tr}\{P[[P, \Lambda_1], [P, \hat{\xi}]]\} \\ &= i \text{Tr}\{P[[P, \Lambda_1], [P, \hat{\xi}]]\} \\ &= \text{Ch}_I(P) \end{aligned}$$

by the same methods used in section 9. □

Lemma 11.4. *Let $u : \mathbb{Z}^2 \rightarrow U(1)$ such that for fixed $b \in \mathbb{Z}^2$*

$$|u(n) - u(n+b)| = \mathcal{O}(|n|^{-1})$$

as $|n| \rightarrow \infty$ ($\|\cdot\|_1$ is the trace-norm). Then

$$[P, \hat{u}] \in \mathcal{L}^3$$

where \hat{u} is the $U(1)$ multiplication operator corresponding to the function u . In particular,

$$P\hat{u}P + P^\perp$$

is a Fredholm operator.

Proof : Fix $n \in \mathbb{Z}^2$. The plan is to compare \hat{u} to $u(n)\mathbb{1}$ in the vicinity of n . We have

$$P\hat{u}P^\perp = P(\hat{u} - u(n))P^\perp.$$

Since P is a gapped Fermi projection there exists a $C < \infty$ and $\mu > 0$ such that

$$\|P_{nm}\|_1, \|P_{nm}^\perp\|_1 \leq Ce^{-\mu|n-m|}.$$

Using the condition on u we find then that

$$\|(P\hat{u}P^\perp)_{n,n+b}\|_1 \leq e^{-\mu|b|/2} \times \mathcal{O}(|n|^{-1})$$

for all $n, b \in \mathbb{Z}^2$. It follows that

$$\sum_n \|(P\hat{u}P^\perp)_{n,n+b}\|_1^3 = \mathcal{O}(e^{-\mu|b|/2})$$

hence

$$\sum_b \left(\sum_n \|(P\hat{u}P^\perp)_{n,n+b}\|_1^3 \right)^{1/3} < \infty.$$

We conclude that $P\hat{u}P^\perp \in \mathcal{L}^3$. By the same argument this holds also for $P^\perp\hat{u}P$, so we have $[P, \hat{u}] \in \mathcal{L}^3$. The operator $P\hat{u}P + P^\perp$ is then Fredholm by Fedosov's formula (proposition 11.3). \square

Lemma 11.5. *Let $G = G^\dagger$ be exponentially local, P a gapped Fermi projection and $[G, P] = 0$. Let $\xi : \mathbb{Z}^2 \rightarrow \mathbb{C}$ such that for fixed $b \in \mathbb{Z}^2$*

$$|\xi(n) - \xi(n+b)| = \mathcal{O}(|n|^{-1}), \quad (185)$$

then

$$[P, e^{iG\hat{\xi}G}] \in \mathcal{L}^3 \quad (186)$$

where $\hat{\xi}$ is the multiplication operator corresponding to the function ξ .

Proof: Fix $n \in \mathbb{Z}^2$. The plan is to compare $e^{iG\hat{\xi}G}$ to $e^{iG\xi(n)G}$ in the vicinity of n . We have by the functional calculus

$$\begin{aligned} A = e^{iG\hat{\xi}G} - e^{iG\xi(n)G} &= \frac{1}{2\pi i} \oint_\Gamma dz e^{iz} \left((z - G\hat{\xi}G)^{-1} - (z - \xi(n)G^2)^{-1} \right) \\ &= \frac{1}{2\pi i} \oint_\Gamma dz e^{iz} (z - G\hat{\xi}G)^{-1} G(\hat{\xi} - \xi(n))G(z - \xi(n)G^2)^{-1} \end{aligned}$$

where the path Γ is a box surrounding the spectra of $G\hat{\xi}G$ and $\xi(n)G^2$, and we used the resolvent identity. Since $G\hat{\xi}G$ and $\xi(n)G^2$ are both bounded and exponentially local with the same decay rate μ , they both satisfy a Combes-Thomas estimate

$$\|(z - G\hat{\xi}G)_{nm}^{-1}\|_1, \|(z - \xi(n)G^2)_{nm}^{-1}\|_1 \leq \frac{2}{|\operatorname{Im} z|} e^{-\mu|\operatorname{Im} z||n-m|} \quad (187)$$

for all $n, m \in \mathbb{Z}^2$ and all $z \in \mathbb{C} \setminus \mathbb{R}$. Also, by the hypothesis on the function ξ , we have that

$$\|(\hat{\xi} - \xi(n))_{ll'}\|_1 \leq \delta_{l,l'} \mathcal{O}(|n|^{-1}) \quad (188)$$

so

$$\|A_{nm}\|_1 = e^{-\mu'|n-m|} \times \mathcal{O}(|n|^{-1}). \quad (189)$$

Now, since $[G, P] = 0$ we have that

$$Pe^{iG\hat{\xi}G}P^\perp = P(e^{iG\hat{\xi}G} - e^{i\alpha G^2})P^\perp \quad (190)$$

and so, using that P and P^\perp are exponentially local,

$$\|(Pe^{iG\hat{\xi}G}P^\perp)_{nm}\|_1 = e^{-\mu''|n-m|} \times \mathcal{O}(|n|^{-1}).$$

We thus have

$$\sum_n \|(Pe^{iG\hat{\xi}G}P^\perp)_{n,n+b}\|_1^5 \leq Ce^{-\mu''|b|} \quad (191)$$

for all $n \in \mathbb{Z}^2$ and so

$$\sum_b \left(\sum_n \|(Pe^{iG\hat{\xi}G}P^\perp)_{n,n+b}\|_1^5 \right)^{1/5} < \infty \quad (192)$$

and it follows that $Pe^{iG\hat{\xi}G}P^\perp \in \mathcal{L}^3$. By the same reasoning also $P^\perp e^{iG\hat{\xi}G}P \in \mathcal{L}^3$, so we conclude that $[P, e^{iG\hat{\xi}G}] \in \mathcal{L}^3$. \square

12 Bulk-edge correspondence for Hall insulators

In this section we introduce the bulk-edge correspondence for Hall insulators and state a theorem expressing this correspondence in the translation invariant case. We do not give the proof, the diligent student is encouraged to dive into the cited literature.

12.1 The physical picture

We have seen that a gapped Hamiltonian gives rise to a gapped Fermi projector to which we can assign an integer Chern number. This Chern number can be computed locally, and gives the same result no matter where we compute it. More physically, this Chern number can be *measured* locally, by measuring the Hall current flowing perpendicular to an applied electric field.

Suppose now you have two materials 1 and 2 described by Hamiltonians H_1 and H_2 , both gapped at zero and giving rise to Chern numbers $\sigma_1 \neq \sigma_2$ respectively. What happens if we stick these two materials together? To investigate this question, let's consider a Hamiltonian H which looks like H_1 to the left of the x_2 -axis and looks like H_2 to the right of the x_2 -axis.

Very far from the x_2 -axis it seems reasonable to assume that the system described by H behaves very much like the system H_1 to the left, and like the system H_2 to the right. In particular we can measure the Hall conductance of H far to the left and far to the right and get σ_1 and σ_2 , two different numbers.

But we proved that if H has a gap at 0 that then the Hall conductance is the same everywhere! We conclude that H cannot have a gap at 0.

The (generalized) eigenstates associated to the spectrum in the gap is obviously associated to the edge between the two materials. This leads us to conclude that this system is an *electric conductor* at the edge!

We can say even more. Suppose $\sigma_1 > \sigma_2$ and apply an electric field as in figure 9. Then the unequal Hall currents result in a pileup of electrons at the edge. From the point of view of the edge this is rather miraculous. It means that applying an electric field seems to create particles out of nowhere!

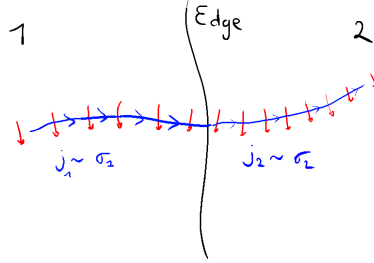


Figure 9: A potential drop across the edge between two Hall insulators leads to a buildup of charge at the edge.

An electric field along a one-dimensional conductor increases the momenta k of all the occupied states, resulting in a picture like in figure 10. The net result is that there are some more particles with momenta near k_1 where the dispersion relation $\omega(k)$ has positive slope, and correspondingly a few less particles with momenta near k_2 where the dispersion relation has negative slope. The net number of particles remains the same. Remembering that the velocity of a wavepacket at momentum k is (up to physical constants) the derivative of the dispersion relation, we see that the net velocity of particles has increased in the direction along the electric field, as expected.

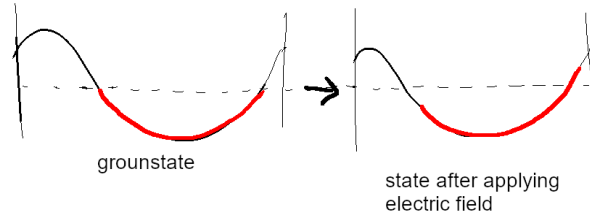


Figure 10: The groundstate of a normal conductor evolves under the influence of an electric field by uniformly increasing the quasi-momenta k

Under normal circumstances the dispersion relation is a periodic function

of k , and for every point where the dispersion relation dives below the Fermi energy there must be another point where it rises above again. This gives a consistent picture of the fact that charge is conserved when an electric field is applied. But suppose that somehow we have a dispersion relation like the one in figure 11. Ignoring for now the question of where the dangling ends of this curve end up, then applying an electric field does seem to create charges out of thin air! A system described by such a strange dispersion relation is called a *Chiral fermion*, and the miraculous phenomenon of charge creation is called the *Chiral anomaly*.

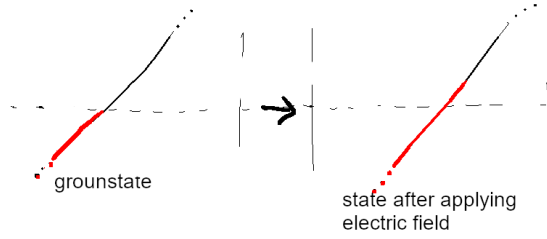


Figure 11: In a chiral conductor, charge appears ‘out of nowhere’ when an electric field is applied!

We are thus led to the idea that the edge between two Hall insulators is chiral, as this would explain nicely the charge generation phenomenon. In this context we also see what to do with the dangling ends of the Chiral dispersion relation, we can just let them dissolve in the bulk spectrum as in figure 12. Let n_+ be the number of times the dispersion relation crosses the Fermi energy with positive slope and n_- the number of times the dispersion relation crosses the Fermi energy with negative slope. We expect that

$$\sigma_1 - \sigma_2 = n_+ - n_-. \quad (193)$$

In the next subsection we state a theorem which makes this picture precise.

(As an aside, such anomalies do occur in the Standard model of elementary particles. This has led some people to speculate that our world is the edge between higher dimensional worlds that are somehow topologically distinct!)

12.2 A theorem

Let H be a translation invariant Hamiltonian on $l^2(\mathbb{Z}^2, \mathbb{C}^N)$ with a spectral gap at zero, and let $P = \chi_{(-\infty, 0]}(H)$ be the corresponding gapped Fermi projection. These data describe the *bulk* of a two-dimensional insulator.

The edge of this insulator is described by a corresponding *edge Hamiltonian* H_E acting on $l^2(\mathbb{Z} \times \mathbb{N}; \mathbb{C}^N)$, where the crystal now fills a half-space $\mathbb{Z} \times \mathbb{N}$, embedded in the full space by

$$\iota : \mathbb{Z} \times \mathbb{N} \rightarrow \mathbb{Z}^2 : (x_1, x_2) \mapsto (x_1, x_2) \quad (194)$$

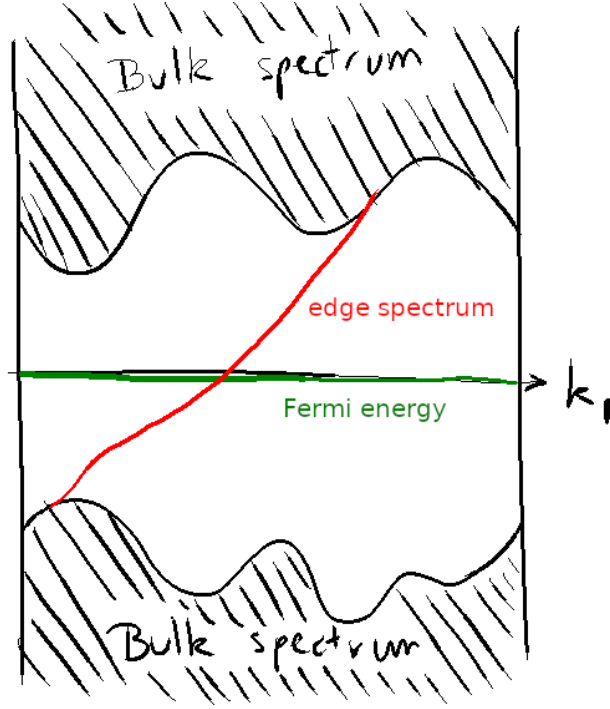


Figure 12: The edge between Hall insulators may be a chiral conductor.

We take $H_E = \iota^*(H)$, which is just the restriction of H to the upper half plane. The Hamiltonian H_E describes the edge between the insulator H and the ‘vacuum’, which of course is a trivial Hall insulator.

Both H and H_E are translation invariant in the 1-direction, so we can take the Fourier transform. We get two norm-smooth maps

$$\mathbb{T}^1 \rightarrow \mathcal{L}(l^2(\mathbb{Z}; \mathbb{C}^N)) : k_1 \mapsto \tilde{H}(k_1) \quad (195)$$

and

$$\mathbb{T}^1 \rightarrow \mathcal{L}(l^2(\mathbb{N}; \mathbb{C}^N)) : k_1 \mapsto \tilde{H}_E(k_1). \quad (196)$$

The spectra $k_1 \mapsto \sigma(\tilde{H}(k_1))$ are essential and are all gapped where H is gapped (because the spectrum of H is the union of the spectra of the $\tilde{H}(k_1)$ ’s). The ‘Hamiltonian’ $\tilde{H}_E(k_1)$ is the restriction to the positive half-line of $\tilde{H}(k_1)$. i.e. we can write

$$\tilde{H}(k_1) = \begin{bmatrix} \tilde{H}_E(k_1) & \Lambda \tilde{H}(k_1) \Lambda^\perp \\ \Lambda^\perp \tilde{H}(k_1) \Lambda & \Lambda^\perp \tilde{H}(k_1) \Lambda^\perp \end{bmatrix} \quad (197)$$

where Λ is the projection on the positive half-line. The off-diagonal blocks are the terms of $\tilde{H}(k_1)$ that couple the left and right half-lines. Since we assumed H to be finite range, these are both finite rank operators, in particular compact.

Thus the diagonal

$$\tilde{H}_E(k_1) \oplus \Lambda^\perp \tilde{H}(k_1) \Lambda^\perp \quad (198)$$

is a compact perturbation of $\tilde{H}(k_1)$. Since compact perturbations leave the essential spectrum unchanged and since $\sigma(A \oplus B) = \sigma(A) \cup \sigma(B)$ we have that

$$\sigma_{\text{ess}}(\tilde{H}_E(k_1)) \subset \sigma_{\text{ess}}(\tilde{H}(k_1)) = \sigma(\tilde{H}(k_1)) \quad (199)$$

Thus whatever spectrum $\sigma(\tilde{H}_E(k_1))$ has in the gap, it must consist of eigenvalues. The function $k_1 \mapsto \sigma(\tilde{H}_E(k_1))$ then looks as in figure 12. By smoothness of $k_1 \mapsto \tilde{H}_E(k_1)$ these eigenvalues trace out smooth curves.

Say these curves cross the Fermi energy n_+ times below and n_- times from above. We then define the *edge index* by

Definition 12.1. *The edge index is defined by the signed number of eigenvalue crossings*

$$\text{index}_E(H) = n_+ - n_- . \quad (200)$$

We define the *bulk index* simply as the Chern number of the bulk Fermi projector:

Definition 12.2. *The bulk index is the Chern number of the Bulk Fermi projector:*

$$\text{index}_B(H) = \text{Ch}(P). \quad (201)$$

With these definitions

Theorem 12.3. *we have Bulk-edge correspondence for Hall insulators:*

$$\text{index}_B(H) = \text{index}_E(H). \quad (202)$$

For proofs and variants of this theorem see for example [7, 13]. For an approach using Fredholm indices see [6].

A Technicalia

Various useful theorems and lemmas.

The following lemma is a slight generalization of lemma 1 of [1].

Lemma A.1. *Let A be a bounded operator on $l^2(\mathbb{Z}^d; \mathbb{C}^N)$ with hopping matrices $A_{x,y} = P_x A P_y$ (P_x is the projector on site x). Then*

$$\|A\|_p = (\text{tr } |A|^p)^{1/p} \leq \sum_{r \in \mathbb{Z}^d} \left(\sum_{x \in \mathbb{Z}^d} \|A_{x+r,x}\|_p^p \right)^{1/p}. \quad (203)$$

Proof : Decompose $A = \sum_{r \in \mathbb{Z}^d} A^{(r)}$ with $A^{(r)} = \sum_{x,y \in \mathbb{Z}^d} A_{x,y} \delta_{x-y,r}$. Using the triangle inequality for the norm $\|\cdot\|_p$ we get

$$\|A\|_p \leq \sum_{r \in \mathbb{Z}^d} \|A^{(r)}\|_p. \quad (204)$$

But

$$\|A^{(r)}\|_p = \|(A^{(r)})^\dagger A^{(r)}\|_{p/2}^{1/2} \quad (205)$$

where $((A^{(r)})^\dagger A^{(r)})_{x,y} = A_{x+r,x}^\dagger A_{x+r,x} \delta_{x,y}$ is block diagonal, so

$$\|(A^{(r)})^\dagger A^{(r)}\|_{p/2}^{1/2} = \left(\sum_{x \in \mathbb{Z}^d} \text{tr}(|A_{x+r,x}|^p) \right)^{1/p} \quad (206)$$

which concludes the proof. \square

References

- [1] M. Aizenman and G.M. Graf. Localization bounds for an electron gas. *J. Phys. A: Mathematical and General*, 31(32):6783, 1998.
- [2] Michael Aizenman and Simone Warzel. *Random operators: disorder effects on quantum spectra and dynamics*. Graduate studies in mathematics. American Mathematical Society, Providence, RI, 2015.
- [3] J.E. Avron, R. Seiler, and B. Simon. Charge deficiency, charge transport and comparison of dimensions. *Commun. Math. Phys.*, 159:399–422, 1994.
- [4] J. Bellissard, A. van Elst, and H. Schulz-Baldes. The noncommutative geometry of the quantum Hall effect. *J. Math. Phys.*, 35(10):5373–5451, 1994.
- [5] A. P. Calderón. The analytic calculation of the index of elliptic equations. *Proceedings of the National Academy of Sciences*, 57(5):1193–1194, 1967.

- [6] A. Sheta A. Wang K. Yamakawa E. Fonseca, J. Shapiro. Two-dimensional time-reversal-invariant topological insulators via fredholm theory. *arXiv:1908.00910 [math-ph]*, 2019.
- [7] M. Porta G. M. Graf. Bulk-edge correspondence for two-dimensional topological insulators. *Comm. Math. Phys.*, 324:851–895, 2013.
- [8] Alexei Kitaev. Anyons in an exactly solved model and beyond. *Annals of Physics*, 321(1):2 – 111, 2006. January Special Issue.
- [9] K. v. Klitzing, G. Dorda, and M. Pepper. New method for high-accuracy determination of the fine-structure constant based on quantized hall resistance. *Phys. Rev. Lett.*, 45:494–497, Aug 1980.
- [10] R. Kubo. Statistical-mechanical theory of irreversible processes. I. General theory and simple applications to magnetic and conduction problems. *J. Phys. Soc. Japan*, 12(6):570–586, 1957.
- [11] R.B. Laughlin. Quantized Hall conductivity in two dimensions. *Phys. Rev. B*, 23(10):5632, 1981.
- [12] Gerard J. Murphy. Fredholm index theory and the trace. *Proceedings of the Royal Irish Academy. Section A: Mathematical and Physical Sciences*, 94A(2):161–166, 1994.
- [13] G. M. Graf P. Elbau. Equality of bulk and edge hall conductance revisited. *Comm. Math. Phys.*, 229:415–432, 2002.